Peripheral Retinal Signals in Human Myopia: A Study of Peripheral Retinal Contours using Biometric and Optical Quality Parameters

A thesis presented to the graduate faculty of
the New England College of Optometry in partial fulfillment
of the requirements for the degree of Master of Science

Gabriella M. Velonias

April 2020

© Gabriella M. Velonias
All rights reserved.

The author hereby grants the New England College of Optometry permission to reproduce and to distribute publicly paper and electronic copies of the thesis document in whole or in part.

Peripheral Retinal Signals in Human Myopia

Gabriella M. Velonias

This manuscript has been read and accepted by the Thesis Examination committee in satisfaction of the thesis requirement for the Degree of Master of Science.

April 21, 2020
Date

Fuensanta A. Vera-Diaz, OD, PhD
Graduate Faculty Advisor

Jane Gwiazda, PhD
Thesis Committee Member

Peter Bex, PhD
Thesis Committee Member

Hilary Gaiser, MS, OD
Thesis Committee Member

April 21, 2020
Date

Jane Gwiazda, PhD
Director of Graduate Studies

New England College of Optometry

Abstract

Peripheral Retinal Signals in Human Myopia –
A Study of Peripheral Retinal Contours using Biometric and Optical Quality Parameters

Background: Human and animal studies suggest that the degradation of retinal image quality across the near retinal periphery disrupts the eye growth stop signal and therefore the emmetropization process. Knowledge of the retinal contour, biometry, and optical properties across the retina is important to understand emmetropization and ultimately for the development of individualized myopia prevention and control treatments.

Methods: 33 young adults (24.12 ± 1.62 years) participated (n=21 myopia, n=11 emmetropia). Central and peripheral axial length (AXL) and monochromatic aberrations were obtained for each subject under different conditions. AXL measurements were taken at 13 eccentricities across the central 40 degrees of the horizontal meridian. Conic functions were fitted to AXL data to analyze their correlations in young adults with emmetropia or myopia. Optical image quality (aberrations) measurements were taken for every degree across the central 50 degrees of the horizontal meridian. Optical quality was computed as the Strehl ratio based on the optical transfer function (VSOTF) to the 5th order for a 4mm pupil. Individual spherical aberration (SA) values were also analyzed.

Biometric Results: Compared to central AXL, peripheral eye length are significantly shorter in myopes creating a more curved ($F=12.067$, $p<0.001$), prolate profile compared to emmetropes. Myopic retinal contours reveal naso-temporal asymmetry with increased curvature at the temporal eccentricities (p ranging from 0.001 to 0.049). The effect of AXL in eccentricity is defined as quadratic function for both myopic ($\eta_p^2=0.60$, $p<0.001$) and emmetropic ($\eta_p^2=0.432$, $p=0.015$) eyes. Accurate AXL fits to a conic function are achieved for most subjects. Myopic eyes show significantly more negative asphericity indicating more prolate, less oblate profiles (Welch statistic 10.323, $F=18.063$, $p<0.01$). There is, however, no effect of refractive error (Welch statistic 0.325, $F = 25.509$, $p=0.574$) or AXL (Pearson $R=0.097$, $p=0.624$) on the apical curvature of the fits.

Optical Quality Results: An overall effect of eccentricity in optical quality is found for all subjects ($F=11.057$, $p<0.001$, $\eta_p^2=0.269$). Myopic eyes show more negative VSOTF values temporally compared to emmetropes, indicating poorer image quality in myopes in this peripheral area. The shape of the overall peripheral optical quality is relatively consistent across refractive groupings and it is best explained with a quadratic fit ($F=32.989$, $p<0.001$, $\eta_p^2 =0.524$), with VSOTF decreasing at a higher rate temporally than nasally. Myopes show more negative SA values than emmetropes on-axis and across the periphery, with the greatest difference in the near periphery ($F=3.765$, $p=0.003$, $\eta_p^2=0.112$). Almost all subjects show peripheral SA shapes best explained with linear fits ($F=13.606$, $p=0.001$, $\eta_p^2 =0.312$), but with a trend towards higher SA values temporally than nasally.

Correlation Results: While there is no correlation on-axis between AXL and VSOTF, peripheral AXL is directly correlated with VSOTF, indicating poorer optical quality with shorter peripheral AXL ($R=-0.111$, $p=0.042$). There is an indirect correlation between AXL and on-axis

SA, indicating a more negative peripheral SA in longer (on-axis AXL) eyes ($R=-0.195$, $p<0.001$).

Conclusions: It is generally agreed that degraded retinal image quality plays a role in the failure of emmetropization; because aberrations degrade image quality is, there is potential to link increased aberrations with myopic progression. We argue that the study of optical quality metrics must be supplemented with the study of biometric parameters; both metrics and their interactions need to be incorporated into models of myopia.

Acknowledgements

Above all, I would like to sincerely thank my faculty advisor, Dr. Fuensanta A. Vera-Diaz, for her consistent support and encouragement over these last few years. Your dedication to optometry and vision science through research, direct patient care, and academic excellence is inspiring, I could not have asked for more a knowledgeable and motivating mentor.

I would like to extend a special thanks to my thesis committee members, Dr. Jane Gwiazda, Dr. Peter Bex, and Dr. Hilary Gaiser, for their time and constructive feedback.

I would like to thank Dr. Ji He for his crucial contribution to this project. He calculated the VSOTF values from the raw aberrometry data. I also must thank Dr. Tony Guarino and Dr. Chris Taylor for their help with structuring and completing statistical analysis for this project.

I thank Enian Kallamata, a great lab mate, colleague, and even better friend.

Finally, thank you to the Graduate Studies Program at the New England College of Optometry, the NEI T35 Program for helping to fund this research.

Table of Contents

Abstract Page i

Acknowledgements Page ii

Table of Contents Page 1

1. General Introduction: **Page 3**
- 1.1 Myopia and Ocular Length Page 3
- 1.2 Retinal Image Quality and the Human Eye's Optics Page 5
- 1.3 The Ocular Periphery Page 6
- 1.4 Study Aims and Hypothesis Page 9

2. General Methodology: **Page 11**
- 2.1 Subjects Page 11
- 2.2 Vision Screening Page 12
- 2.3 Experimental Data Page 13

3. Ocular Contours – Biometry: **Page 14**
- 3.1 Background Page 14
- 3.2 Methodology Page 17
  - 3.2.1 Procedures Page 18
  - 3.2.2 Subjects Page 18
  - 3.2.3 Data Processing and Analyses Page 19
- 3.3 Results Page 21
  - 3.3.1 Biometry Raw Data Page 21
  - 3.3.2 Conic Fittings Page 24
- 3.4 Discussion Page 26

4. Peripheral Optical Contours – Aberrations **Page 30**
- 4.1 Background Page 30
- 4.2 Methodology Page 34
  - 4.2.1 Procedures Page 34
  - 4.2.2 Subjects Page 36
  - 4.2.3 Data Processing and Analyses Page 37
- 4.3 Results Page 38
  - 4.3.1 Overall Optical Image Quality Page 39
  - 4.3.2 Spherical Aberration Page 40
- 4.4 Discussion Page 42

5. Comparison of Peripheral Biometry and Optical Contours: **Page 46**
5.1 Background Page 46
5.2 Methodology Page 48
5.3 Results Page 48
5.4 Discussion Page 50

6. General Conclusions **Page 52**

7. Appendix 1: Raw Data **Page 55**

8. Appendix 2: ARVO 2019 Posters **Page 57**

9. References **Page 59**

1. General Introduction

1.1 Myopia and Ocular Length

Myopia is a highly prevalent disorder labelled as a major public health concern achieving epidemic status in certain East Asian countries(1,2). Worldwide, refractive errors (RE) are the most common cause of visual impairment and the second leading cause of vision loss(3). Myopia presents specific risks for visual impairment and potentially blinding ocular diseases(4), decreased quality of life(5), limited educational and occupational opportunity(6), and heavy economic burden measured in billions of dollars(7,6). Myopia is typically defined as a minimum of -0.50D spherical equivalent refractive correction with the definition shifting to high myopia at -5.00D or worse in either eye (or greater than 26mm axial length, AXL)(7). Myopic consequences begin at levels as low as -1.50D leading to pathological sequelae or avoidable vision loss and blindness(7). All patients with myopia should have access to accurate and appropriate optical correction, however, this does not address the excessive ocular growth and pathological consequences. The World Health Organization currently lists myopia as one of the five ocular disorders of highest priority. By 2050, an alarming 50% of the world's population is predicted to have myopia, when in 2010 it was merely 28%(7). This unprecedented rapid rise in myopia worldwide along with the younger ages of onset imply genetics cannot solely be responsible. Myopia is a multifactorial with both genetic and environmental factors contributing to its development and progression, emphasizing the need to research environmental causes. Additionally, the economic impact is measured in billions of dollars(7). Myopia presents a threat to global health; as such comprehensive eye care to correct the refractive error with spectacles and contact lenses and manage the resultant ocular sequelae is essential but not enough. There is

a need for a better understanding of not only the mechanisms of myopia but also successful interventions to slow its progression or halt development.

Myopia is caused by increased axial elongation that does not correspond to the eye's optical power. The length of the eye is longer than the focal length of its optics resulting in a retinal image that falls in front of the retina. This abnormal axial elongation is caused primarily by an increase in vitreal chamber depth(8). Excessive ocular enlargement(9), in concert with shear force from vitreous motion during eye movements(10), may create a mechanical demand on the retina causing retinal thinning(11). The enlarged length along the optic axis in myopic eyes results in a prolate retinal contour with central myopia and relative peripheral hyperopia. The increased retinal stress may manifest as degenerative diseases such as myopic maculopathy, non-rhegmatogenous retinal detachment, or primary open angle glaucoma(12).

Emmetropization is the mechanism whereby the eye grows to match its optical components, beginning as low hyperopia in infancy and progressing to emmetropia (absence of refractive error) in early childhood(13). It is established that eye growth during development is regulated by visual feedback, particularly retinal image quality(14,15). It appears that while corneal and lens growth are mostly genetically pre-programmed, retinal response driven ocular elongation is much more complex(14,15). Normally during childhood, scleral growth from retina-driven cues in concert with the flattening of the cornea and crystalline lens combine to match the eye's optical power leading to emmetropia. However, in many individuals, abnormal visual stimuli interfere with this process creating refractive error. In general, it is widely agreed upon that eye growth is visually guided, however the specific signals driving refractive error development are unknown. There is extensive evidence that lens-induced optical blur generates refractive error(16–19). Even more interesting is that animal models have shown partial or

complete refractive recovery with the use of optical defocus (exposure to positive lenses)(16–19). High power convex lenses in chick and other animal models induce hyperopia whereas high power concave lenses lead to myopia. Most notably, partial or complete recovery from myopia has been observed with the use of myopic defocus (positive lenses) in some models, including chicks and tree shrew(20–22). However, these findings are not transferrable to humans; foveal myopic defocus does not arrest the progression of myopia in humans. In this study, we strive to evaluate specific aspects of the retinal image quality associated with human myopia.

1.2 Retinal Image Quality and the Human Eye's Optics

The eye's optical image quality and its degradation is determined by the interaction of optical aberrations in our visual system. The main source of aberrations is derived from imperfections in two ocular tissues: cornea and lens. The optical image quality, derived from waterfront measures, can be experimentally measured to indicate the quality of the retinal image. The optical wavefront, the surface formed by joining the leading edges of all light rays, takes on an irregular, aberrated shape at the retina.

Ocular wave aberrations are typically represented by Zernike polynomials(23). The wavefront shape is the result of all Zernike polynomials, each with weighted values. It is important to emphasize that all optical aberrations, not just low order (sphere and cylinder), affect the retinal image quality. Any Zernike coefficient of order three or higher is referred to as higher-order aberrations.

Reduced retinal image quality is not, on its own, a problem for the visual system. Blurred retinal image quality drives the human accommodative response allowing for the resolution of fine details and near tasks(30,31). Additionally, blur provides depth cues and spatial awareness

in the environment(32,33). However, degraded image quality is also thought to be a causative factor in myopic eye growth(13).

Defocus, astigmatism, coma, and spherical optical aberrations have the largest effect on the retinal image quality(24–27). Peripheral blur is dominated by defocus and oblique astigmatism. Defocus degrades image quality the most, however, oblique astigmatism varies the most as a function of eccentricity thus its impact dominates in the periphery(23). Porter et al(28) reported that defocus and astigmatism account for over 92% of the total wavefront aberration variance. The study of spherical aberration (SA) is important, even if it degrades the retinal image to a lesser extent, because of its possible association with myopia(28, 29). While aberrations decrease in magnitude as order increases, SA is an exception and has a larger impact than any other fourth or third order aberrations(28).

Generally, the higher the order of the optical aberration, the weaker the effect on image quality particularly in the setting of small pupils(34). Such higher-order aberrations become significant when observing the visual performance of an ocular system with large or dilated pupils. Nevertheless, the study of ocular aberrations necessitates the consideration all aberrations as a group; this is because combinations of aberrations improve retinal image quality compared to isolated aberrations(35,36). Our study measures the optical image quality of each subject both on-axis and in the periphery.

1.3 The Ocular Periphery

Studies with animal models have provided strong evidence for the role of peripheral image quality on myopia development. In some such models, including primates, local retinal signals either at the fovea or other locations in the peripheral retina cause myopic development

and eye growth(37). For example, rhesus monkeys can still emmetropize when their central retinae are ablated or blocked; but if there is interference with the peripheral retina, less peripheral hyperopia and central myopia results(15,38,39). Clinical work in humans also supports the idea that the peripheral retina alters refractive development. In 1971, Rempt et al(40) showed that while there is relative myopic refraction in the periphery of emmetropic and hyperopic eyes, myopic eyes show relative peripheral hyperopia. That same year, Hoogerheide et al(41) proposed that emmetropes and hyperopes with relative peripheral hyperopic astigmatism had a greater risk of myopia development. Additionally, researchers found that disruption to the peripheral retina well outside the central retina, such as retinopathy of prematurity or retinitis pigmentosa, laser photocoagulation, and peripheral cryotherapy can be associated with central refractive error development(42,43). Early human studies, animal studies, and clinical trials propagated the claim that peripheral hyperopia is a determinant for future myopic refractive error. However, recent and robust evidence now shows that this is too simplified. Indeed, the peripheral relative hyperopia pattern found in myopic eyes is a consequence of myopia, rather than a cause(44). A large scale, longitudinal study examining 7 to 14 year-old Chinese children (n=2134 and n=1780, respectively) concluded that relative peripheral hyperopia is a consequence rather than a predictor of change in central refraction. They(44) further provided a plausible explanation as to why the peripheral optics may not be relevant in the development and progression of myopia. If the hypothesis held true then relative peripheral hyperopia would cease to promote myopic growth when the myopic child were uncorrected, which is not the case(44). Closer investigation by Rosen et al(45) into the methodology of Hoogerheide et al(41) disproves the evidence that peripheral refractive status predicts myopia development. The authors(41) reasoned that peripheral refractions were measured at a later examination than central refractions

and once myopia had already developed or not. A study duration of 10-15 years would have been needed otherwise. Additionally, a 12 month longitudinal study by Lee and Cho(46) found no correlation between myopic shift and relative peripheral refraction in Chinese children aged six to nine years. Sng et al(47) conducted a similar study of greater power, all 187 seven year old children in their study had baseline peripheral myopia. After 15 months, some children developed myopia with peripheral hyperopia, while others remained emmetropic with peripheral myopia(47).

These conclusions do not, however, dismiss the effect of peripheral vision on the risk to develop myopia. It is widely accepted that retinal image quality across the periphery, not only at the fovea, plays a significant role in myopia development(14,37,38,49). However, it is not yet understood what retinal image qualities or what specific areas are important to this process.

There are specific areas of the retina that show larger differences in refraction, biometry values, and optical image quality between emmetropes and myopes and are therefore worth further investigation. The largest difference between myopic and emmetropic eyes appears to lie in the near peripheral retina, 20 degrees nasally and 15 degrees temporally from the fovea(37,50). Outside this range, retinal image quality is similar for eyes with all types of refractive error, likely because oblique astigmatism degrades peripheral retinal image quality in emmetropes and hyperopes but has a compensatory effect in myopes(23). The near peripheral retina should be investigated further not only because of its differences amongst refractive groups but also because the human retina decoding system for optical blur appears to be located in the retinal near periphery rather than the fovea(51,53). Recent evidence using electrophysiology has pointed to the near periphery up to 15 degrees as the human retina decoding system for blur(54). Chin et al(51) found a larger increase in multifocal

electroretinography (ERG) amplitude para-centrally (up to 12 degrees of eccentricity) compared to centrally when blur stimuli were introduced. Our lab(55) also found differences in pattern ERG responses to blur presented at various eccentricities, indicating that the retinal area driving blur is within 6 and 12 degrees eccentricity. This human retinal decoding system for optical defocus is not only noted to be located in the near periphery but also seems to be tuned for low to mid spatial frequencies. For example, defocus serves as a cue for accommodative response, but this does not only occur centrally, as expected, but also in the near periphery(56,57). Interestingly, myopic individuals reveal less effective control over peripheral accommodation than emmetropes(58). Our lab(59) also found that the effect of central attention in peripheral vision also varies in myopia compared to emmetropia. Myopes experience a decrease in contrast sensitivity in the far periphery (30 degrees) compared to emmetropes when doing near tasks. No difference was observed in near peripheral ranges (8-17 degrees)(59).

1.4 Study Aims and Hypothesis

The research presented in this thesis comprises three separate chapters: the study of biometric ocular shape data (AXL), the study of optical quality data (VSOTF), and the correlation of both results. These three chapters together address components of anatomical and optical properties in myopes that are not yet well understood. It is a detailed study of structure and function in human myopia that attempts to explain what specific aspects of the retinal image quality are associated with human myopia. We will show the importance of studying the retinal near periphery in myopia and support our hypothesis that there is significant individual variability of retinal profiles and image quality. Individual correlations of retinal image quality with biometric parameters will also be more variable in myopic eyes. Only the horizontal

meridian results for the right eye are reported here, however we have data along the vertical data constituting a 40x30 2D map of biometric data and a 50x30 2D map of retinal image quality which will be prepared for a near future paper publication. This thesis is the first stage of a larger study aimed to develop individual optical correction and 3D digital therapies to slow progression of existing myopia and attempt to prevent myopia in children at risk.

Towards this general purpose, the specific aims of my studies are:

Specific Aim 1 - To study retinal contours determined by fitting conical functions to measured ocular length (based on AXL) across the central 40 degrees in individuals with emmetropia and myopia, and to evaluate the effect of varying degrees of myopia as well as variations with eccentricity in the nasal and temporal meridians.

Specific Aim 2 - To study optical quality, i.e., ocular aberrations, across the central 50 degrees in individuals with emmetropia and myopia, and to evaluate the effect of varying degrees of myopia as well as variations with eccentricity and nasal and temporal meridians.

Specific Aim 3 - To compare the wide-field two-dimensional data of ocular shape (AXL) with the high-resolution optical quality (VSOTF) in individuals with emmetropia and myopia.

2. General Methodology

2.1. Subjects

A total of 35 young adults (mean ± SD age: 24.12 ± 1.62 years) were recruited from students at the New England College of Optometry to participate in the study. Following a vision screening that comprised an ocular health evaluation and an ocular history questionnaire, 35 subjects who met all inclusion criteria were enrolled. Inclusion criteria required subjects to meet the following: (1) 18-30 years of age, (2) no more than 1.25 D astigmatism in either eye, (3) no more than 0.75 D anisometropia, (4) best corrected LogMAR VA = 0.0 (20/20 equivalent) or better each eye, (5) no history of amblyopia, binocular vision or accommodative abnormalities, or ocular surgery or disease with potential visual consequences, (7) adequate hearing, language skills, and mental ability to understand the consent process and the instructions given during the experiment.

Subject refractive error was determined by open-field autorefractor (Grand Seiko WR500K, Grand Seiko, Hiroshima, Japan, http://www.grandseiko.com/) and finalized with non-cycloplegic binocular subjective refraction. Subjects were divided into two refractive groups. Myopes (n = 21) were defined as having a spherical-equivalent (SE) in the right eye starting at -0.75 up to and including -6.00D (mean central SE: -3.30 ± 1.51D). Emmetropes (n = 12) were defined as having a SE in the right eye starting at +0.25D up to and including -0.375D (mean central SE: -0.03±0.26 D). Two subjects recruited for the study were excluded from further analysis due to their SE refractive error falling between -0.375 and -0.75. Of the 33 subjects, there were four males and 29 females. Of the 33 subjects, 18 identified as Caucasian and 15 were Asian. Because of previous research identifying differences based on the region of Asia, I would like to mention that seven of the 15 identified as East Asian, and eight identified as South Asian.

The study followed the tenets of the Declaration of Helsinki. Informed consent was obtained from all subjects after explanation of the nature and possible consequences of the study, and was approved by the New England College of Optometry's Institutional Review Board. Once the Informed Consent Form was signed, a de-identifier form was completed and subjects were assigned a study number. This study number, with no identifiable information, was used from that point onward.

2.2. Vision Screening

A vision screening, with emphasis on ocular history, refraction, and binocular and accommodative assessment, was conducted to determine a subject's eligibility. Tests performed included:

1. Visual acuity (VA) for each eye using a computerized LogMAR chart at 6m and the NECO LogMAR letters near card at 40cm. Subjects wore their habitual eyeglasses correction, when indicated. Results were recorded in LogMAR units.
2. Estimated cover test at distance and near, with habitual optical correction.
3. Open-field autorefractor objective evaluation of refraction.
4. Subjective refraction to refine the objective measures with binocular balance using a computerized LogMAR chart at 6m.
5. Slit lamp examination of central media clear of opacities: cornea, crystalline lens and vitreous.

2.3 Experimental Data

Once it was determined that the subject met all the inclusion criteria and the refractive group classification, we continued with experimental testing, including:

1. Biometric measures (AXL, corneal curvature, corneal thickness, anterior chamber depth, crystallin lens thickness, vitreous chamber depth) using a Lenstar LS900 (Haag Streit AG, Koeniz, Switzerland, http://www.haag-streit.com/). Results and analysis presented Chapters 3 and 5.
2. Optical quality across the eye using a peripheral scanning Hartmann-Shack wavefront analyzer (scanning peripheral aberrometer, VopticaSL, https://voptica.com/). Results and analysis presented Chapters 4 and 5.
3. For corneal topography, we obtained corneal curvature profiles by scanning the anterior cornea three times per eye using our Oculus Pentacam. Results not presented in this thesis.
4. The MM6 retinal program of the RTVue OptoVue OCT captures 12 retinal slices 6mm by 6mm. Results not presented in this thesis.

3. Ocular Contours – Biometry

3.1. Background

Although myopic eyes are largest in all structural dimensions, including equatorial, anterior-posterior, and vertical axes, the main structural difference in these eyes is AXL. Increased axial elongation in myopia is contributed primarily by the enlarged vitreal chamber depth, but also minimally by the increased anterior chamber depth(8). As a result of this elongation, ocular dimensions between myopes and emmetropes vary considerably.

Magnetic resonance imaging (MRI) is a technique that can be used to describe linear dimensions of ocular shape facilitating a detailed three-dimensional investigation of the eye. Using MRI, the average dimensions for emmetropic eyes are 23.0 ± 0.7mm in length, 22.4 ± 1.0 mm in height and 22.7 ± 0.9 mm in width(60). It was also with MRI that Nagra et al(61) found a larger retinal surface area in the superior temporal quadrant of the human retina compared to any other quadrant, especially inferior nasal. Particularly in myopes, the increased AXL in the superior temporal retina stretches the most, which interestingly is the hypothesized reason for the increased propensity of retinal breaks in this quadrant(61).

Adult linear dimensions of ocular shape increase with myopia at a rate of approximately 0.35mm/D in length, 0.19 mm/D in height, and 0.10 mm/D in width(60). In contrast, with children, the change in AXL is not constant throughout childhood. Change in myopia averages 0.28mm/D at ages 6-7, 0.32mm/D at ages 12-13, and 0.35-0.40mm/D in adults(62). Once myopic, children progress at an average of 0.50mm/D, specifically 0.32mm/D in mild myopia and 0.58mm/D in moderate amounts of myopia(62,63).

Emmetropic eyes have similar AXL, ocular height, and width dimensions with minimal interindividual variability. On the other hand, myopes have the greatest expansion axially,

compared to changes in height or width, and with significant interpersonal variability(60). The ratio between axial elongation compared to heights and widths in myopes ranges between 2:1:1 and 3:2:1, depending on the study methodology(64–67). This ratio suggests that an axial elongation model for myopia development is more applicable compared to a global expansion model. This expansion is possibly a consequence of the bony orbital walls, which provide anatomical constraints. Atchison et al(60) found that using MRI in a population of 88 emmetropes and myopes, the axial elongation model fit 47% of the myopic eyes compared to 18% that fit the global expansion model. This ratio also suggests that transverse and axial growth is regulated differently. Regardless, to date, no one expansion model has been identified to define all myopic eyes. It is likely that there are multiple expansion models at work in both regulated and excessive eye growth.

The use of MRI to determine ocular shape has been devalued due to high costs, long testing times, and low resolution (0.15mm)(60). This technique now serves to validate alternative, less cumbersome, methods of determining retinal shape. Previously, researchers used peripheral refraction to infer ocular and retinal shape. For example, relative peripheral hyperopia was assumed to be equivalent to the shortening of axial lengths into the periphery creating a prolate shape in myopic eyes. As such, an alternative determinant of ocular and retinal shape is the study of refractive errors in the periphery, a technique documented in over 60 publications(68,69). Peripherally, myopes exhibit relative peripheral hyperopia while emmetropes and hyperopes shift towards relative peripheral myopia (70). In addition, peripheral refractions exhibit retinal asymmetry, with the temporal retina showing greater refractive changes than the nasal retina(71,72). While peripheral refraction, can infer eye shape, it does not present a comprehensive retinal contour model. Alternative methods that combine optics,

biometry, and refraction are necessary. Therefore more recent studies have used biometric measurements to model ocular shape.

Partial coherence interferometric (PCI) instruments such as the IOLMaster (Zeiss Meditec) or Lenstar (Haag-Streit AG) are non-contact, reliable, and commercially available devices that can be used to estimate retinal shape up to 30 degrees into the periphery(73). However, they cannot be used on eyes with irregular shaped retinas or optical distortions(73). These instruments provide good resolution at 0.01-0.02mm; this is considerably better than that of the MRI at 0.15mm(73). AXL and interocular parameters obtained with these PCI instruments may be fitted to conic functions to estimate the retinal contour. Using an off-axis PCI method for determining retinal shape was validated against the MRI by Atchison et al with good agreement at 4% error along the horizontal meridian. Additionally, accuracy is not significantly affected by refractive group(74). However, as with any PCI method, certain assumptions are inevitable. The Lenstar relies on a single index of refraction throughout the eye(74). Determining retinal shape from the PCI method is accurate up to approximately 30-40 degrees in each direction from center(68,73). While the PCI method serves as an excellent alternative to the MRI, it does not combine the retinal position with the anterior optical properties of the eye(68). Specifically, on-axis (i.e. 0 degrees) was measured using central fixation. However, this is not necessarily the exact location of the fovea due to angle kappa.

For this study, we utilized the PCI method to determine eye shape, specifically measuring AXL, curvature, and asphericity, as it provides high resolution. Regardless of the method used, it is well documented that myopic eyes are more prolate, or less oblate, compared to emmetropic eyes(68,70,75,76). This is because retinal stretching in myopia forms a prolate ellipsoid surface that is greatest at the posterior pole and flattens out towards the periphery with eventually similar

shapes at large angles for all refractive groups(8,9). The subject of retinal shape as a potential predisposition to myopia progression remains controversial which will be illustrated in the discussion. Ultimately, we identified a need for studies of retinal shape measures in a setting where the optics of the eye are considered as well(70), explored in Chapter 4 and 5.

In this first part of our studies, we report on the ocular shape as determined by ocular biometric properties using a PCI method. We report the AXL values across the central 40 degrees of the horizontal meridian in eyes with emmetropia and various degrees of myopia. We also report differences between temporal and nasal eccentricities. These results will expand the current knowledge of the ocular shape in myopia and emmetropia. The findings will help determine the potential role of ocular shape in myopic development and begin to identify the role of retinal regions/meridians. Finally, a comparison will be made in Chapter 5 between the biometric ocular shape results of this chapter and the optical quality of the eye presented in Chapter 4.

3.2. Methodology

3.2.1 Procedures

Central and peripheral AXL measurements were performed using a Lenstar LS900. Biometry measurements were taken across 13 points out of the central 40 degrees of the transverse (axial) section: 20 degrees, 16 degrees, 12 degrees, 8 degrees, 4 degrees, and on-axis (0 degrees). Peripheral eccentricities were measured by directing the subject's fixation using a custom designed target (Figure 3.1.). Noteworthy, eye rotation does not affect accuracy of peripheral AXL data(1). Three sequential measurements were taken following complete blinking between captures and averaged for each location.

Inherent limitations to the Lenstar optical coherence biometer include the use of a constant index of refraction to evaluate the dimensions of the various surfaces throughout the eye. Rather than using the physiological index of refraction of each media, including the cornea, anterior chamber, or the various depths of the crystalline lens, the instrument produces one overall eye refractive index. As a consequence, the optical path lengths between anatomical boundaries and the overall AXL results are not the true physical pathways but rather instrument specific calculations(1). Additionally, the instrument measures AXL from the front surface of the cornea to the RPE and then the eye length to the retina inner limiting membrane is automatically adjusted assuming a constant retina thickness of 200μm. We induce different eccentricities by directing the subject's fixation during all biometric measures(73,74,78,79). Because eccentricities were induced via fixation targets it is important to note that on-axis 0 degrees was not necessarily the exact location of the fovea due to angle kappa.



Figure 3.1. Transparent, non-accommodative, target used to induce the peripheral eccentricities along the horizontal and vertical meridians, as described in the text.

3.2.2. Subjects

35 subjects completed the study. Two subjects (SE -0.625D) were excluded from further analysis as they did not meeting the refraction criteria for either emmetropia or myopia.

The AXL data for all remaining subjects (33 total) were analyzed (Table 3.1).

Subject ID	Age	Race	Sex	Refractive grouping	On-axis AXL	On-axis SE
PBM001	23	Caucasian	F	Myope	25.15	-4.5
PBM002	23	Caucasian	F	Myope	24.33	-3.875
PBM003	23	East Asian	M	Emmetrope	22.71	0.25
PBM004	24	South Asian	F	Emmetrope	23.85	-0.25
PBM005	22	South Asian	F	Myope	24.1	-1.5
PBM006	23	Caucasian	F	Myope	23.85	-2.75
PBM007	23	East Asian	F	Emmetrope	22.66	0
PBM008	26	East Asian	M	Myope	25.23	-1.75
PBM009	23	Caucasian	F	Myope	25.43	-6
PBM011	24	Caucasian	F	Emmetrope	23.02	0.125
PBM012	25	Caucasian	F	Myope	24.06	-2.5
PBM013	28	Caucasian	F	Emmetrope	23.71	0
PBM014	23	Caucasian	M	Emmetrope	23.13	-0.25
PBM015	24	Caucasian	F	Myope	23.61	-1
PBM016	23	Caucasian	F	Myope	24.49	-2.5
PBM017	28	Caucasian	M	Myope	24.82	-3
PBM019	24	South Asian	F	Emmetrope	24.03	-0.375
PBM020	23	South Asian	F	Myope	24.68	-1.5
PBM021	25	South Asian	F	Myope	24.69	-3.875
PBM022	26	Caucasian	F	Myope	23.55	-2
PBM023	28	East Asian	F	Emmetrope	23.97	-0.5
PBM024	24	East Asian	F	Myope	25.75	-4.375
PBM025	24	South Asian	F	Emmetrope	23.55	0.25
PBM026	25	East Asian	F	Myope	25.74	-4.25
PBM027	23	Caucasian	F	Emmetrope	23.97	0
PBM028	25	Caucasian	F	Myope	24.76	-5.375
PBM029	24	Caucasian	F	Myope	25.26	-3.75
PBM030	24	East Asian	F	Myope	23.85	-4.875
PBM031	22	Caucasian	F	Myope	22.86	-2.5
PBM032	22	South Asian	F	Emmetrope	22.38	0.25
PBM033	24	Caucasian	F	Emmetrope	23.97	0.125
PBM034	25	Caucasian	F	Myope	24.74	-5.75
PBM035	23	South Asian	F	Myope	24.29	-1.625

Table 3.1. The refractive characteristics, age, sex, race, and on-axis results for the right eye of all 33 of the subjects used in the biometric portion of this study.

3.2.3. Data Processing and Analyses

Using Statistical Package for the Social Sciences (SPSS, IBM, Chicago IL, USA), linear regression analysis was performed for the raw data AXL measures at the 13 horizontal specific eccentricity points. Right eye data is presented. Pillai's trace was applied to all multivariate data to evaluate the interaction between eccentricity, AXL, and refractive group using F statistics and p values. Linear interpolation was needed for five subjects. For relationships between different eccentricities within the same refractive group, pairwise Bonferroni functions were applied when needed.

The raw AXL data from the 33 subjects were then imported into Matlab (Statistics Toolbox Release 2012b, The MathWorks, Inc.) to fit the conic function used to fit ocular contours, as described by Verkicharla et al(80), $y_r = AXL'_p - r_{cv}\sin\theta$ and $\Delta z_3 = r_{cv}/(1-\cos\theta) + AXL'_p\cos\theta - AXL'_a$. The off-axis PCI method used in this study was a variant of the Le Grand model eye involving a basic model eye without surface ray deviations. The anterior corneal surface was a constant of 7.8mm radius of curvature. This model assumes no light deviation within the eye and is considered accurate as long as the subject does not have irregular corneas or refractive myopia(74). This method has been previously validated with MRI with good agreement of 3.8±0.7% along the horizontal meridians(74). Theoretical work with this model was found to be highly accurate up to 40 degrees into the periphery(73). The equation used for biometry fittings was:

$$y = C * \frac{(x)^2}{(1 + \sqrt{1 - (1+Q) * C^2 * (x)^2})}$$

where y is surface sag co-ordinate, C is vertex curvature, Q is asphericity, x is the AXL co-ordinate along the X-axis. Note that for biometry fittings there was no need to add an offset (x0, y0) as biometry data was centered around (0,0) in all cases.

Fitting functions were created in Matlab to determine the goodness of fit for each subject's AXL data as well as the overall asphericity and curvature of the fit for each subject. Accurate biometric fittings were defined as goodness of fit (r^2) values 0.70 or higher. Ocular surfaces are described by a family of concoids, conic sections rotated about the principal meridians. To quantify the differences in retinal shape between subject's eyes, two main characteristics were described: radius of curvature (C) and asphericity (Q). C is intuitive as a greater C value indicates a larger radius of curvature and thus a flatter contour. Q values are sign-dependent. A 0 Q value indicates a perfect sphere. A positive Q value indicates a oblate contour while a negative Q value indicates a prolate which eventually can extend to a parabolic shape.

Biometric fittings were analyzed with one-way ANOVAs to evaluate asphericity and curvature for those subjects with good fittings (n=28), defined as goodness of fit >70%. Tests of homogeneity were performed to identify differences in standard deviations within refractive groups.

3.3. Results

3.3.1. Biometry Raw Data

The average on-axis (0 degrees) AXL were 24.54±0.76 mm for myopes and 23.41±0.60 mm for emmetropes. Figure 3.3 shows central eye length measurements with corresponding central refractive error for each subject. As previously reported, there was a strong significant correlation between central refractive error and on-axis AXL ($F=11.828$, $p<0.001$), eyes with higher amounts of myopia are longer (Figure 3.1.a.). Because there is literature to support a difference in AXL values by sex(124) where females have shorter and smaller eyes than males

with the same refractive group, Figures 3.1.b. and 3.1.c. plot the results by sex. Given the small sample size (four males), no further statistical analysis was pursued.

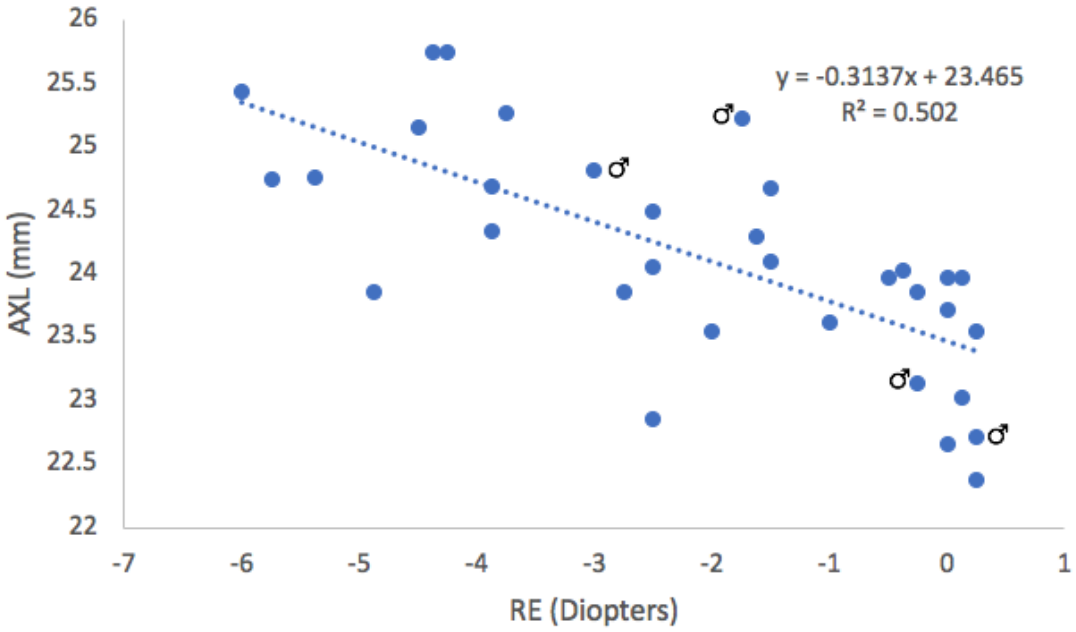


Figure 3.1.a. RE plotted against on-axis AXL values for all subjects. The four males in the study are marked (♂).

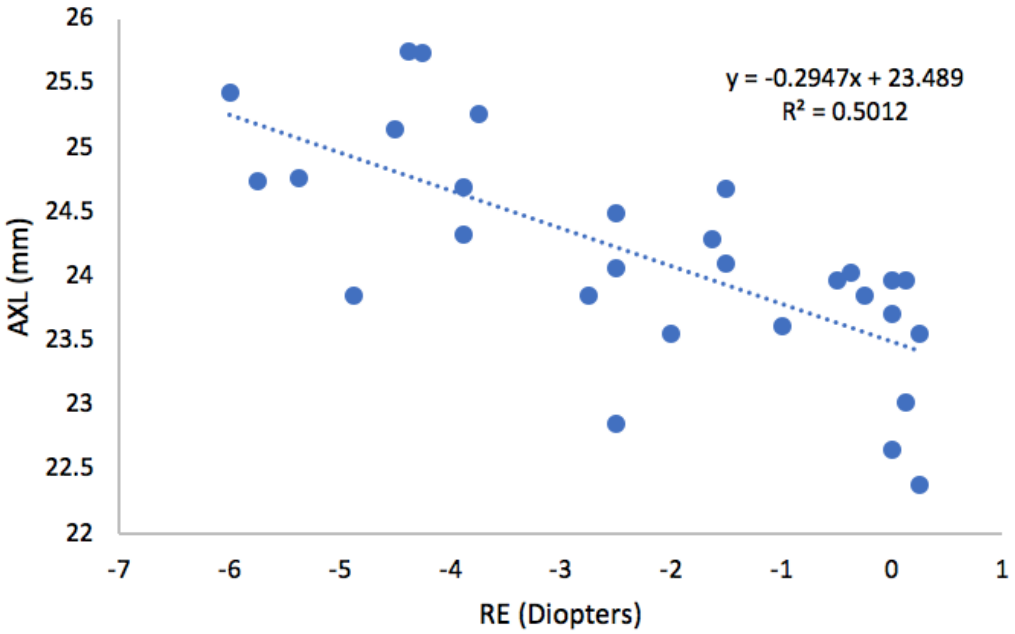


Figure 3.1.b. RE plotted against on-axis AXL values for females.

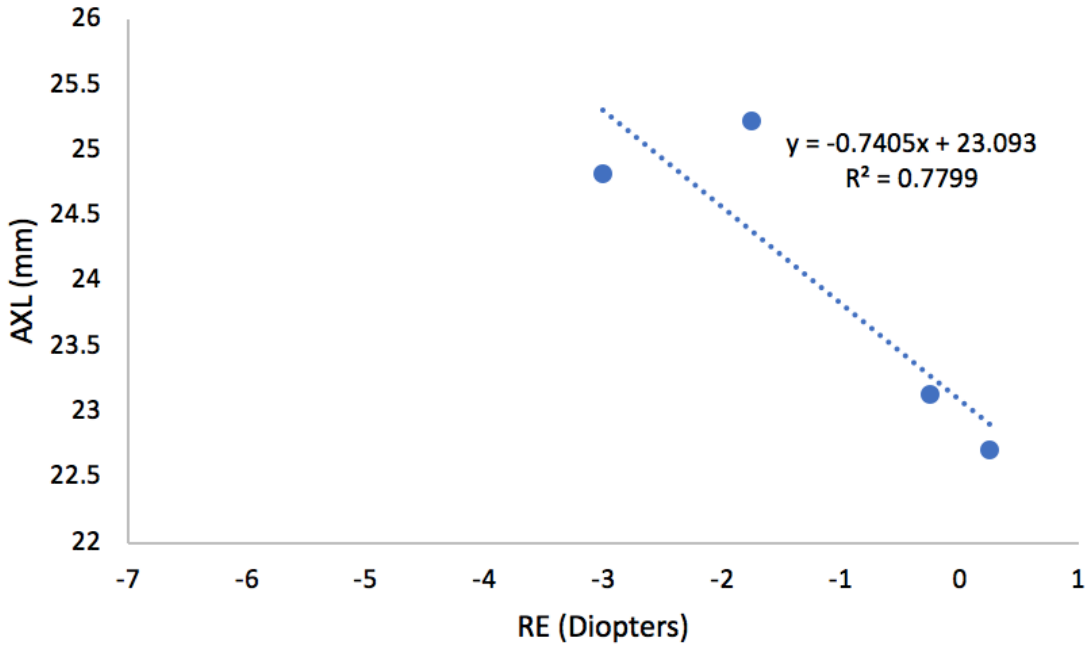


Figure 3.1.c. RE plotted against on-axis AXL values for males.

Across the horizontal periphery, there was a significant main effect of eccentricity and AXL ($F=11.828$, $p<0.001$) for all subjects; as expected, peripheral AXL values were shorter than central AXL. No differences in the effect of eccentricity on the effect of peripheral AXL was found between the two refractive groups ($F=1.360$, $p=0.261$). Specifically, there was a significant effect of AXL by eccentricity in this group of myopes ($F=12.067$, $p<0.001$) but there was not a significant effect of eccentricity and AXL was found in emmetropic subjects ($F=2.872$, $p=0.286$). Unlike emmetropic eyes, myopic AXLs shortened significantly as they extend outwards towards the periphery thus creating a more curved profile compared to emmetropes. A more curved ocular profile was apparent for temporal than nasal eccentricities in myopic eyes. This naso-temporal asymmetry across the horizontal meridian of the myopic subjects showed significance starting at 4 degrees temporal and extending out to 20 degrees temporal (p values ranging from 0.001 to 0.049), proving that differences in ocular shape are not just in the mid or

far periphery but as close as 4 degrees from on-axis. Figure 3.2 shows the mean eye length measurements with 95% confidence intervals of emmetropes and myopes along the horizontal meridian.

The effect of AXL in eccentricity for the central 40 degrees measured was defined as a quadratic function for both myopic (60.0% eta squared, p=0.00) and emmetropic (43.2% eta squared, p=0.015) eyes.

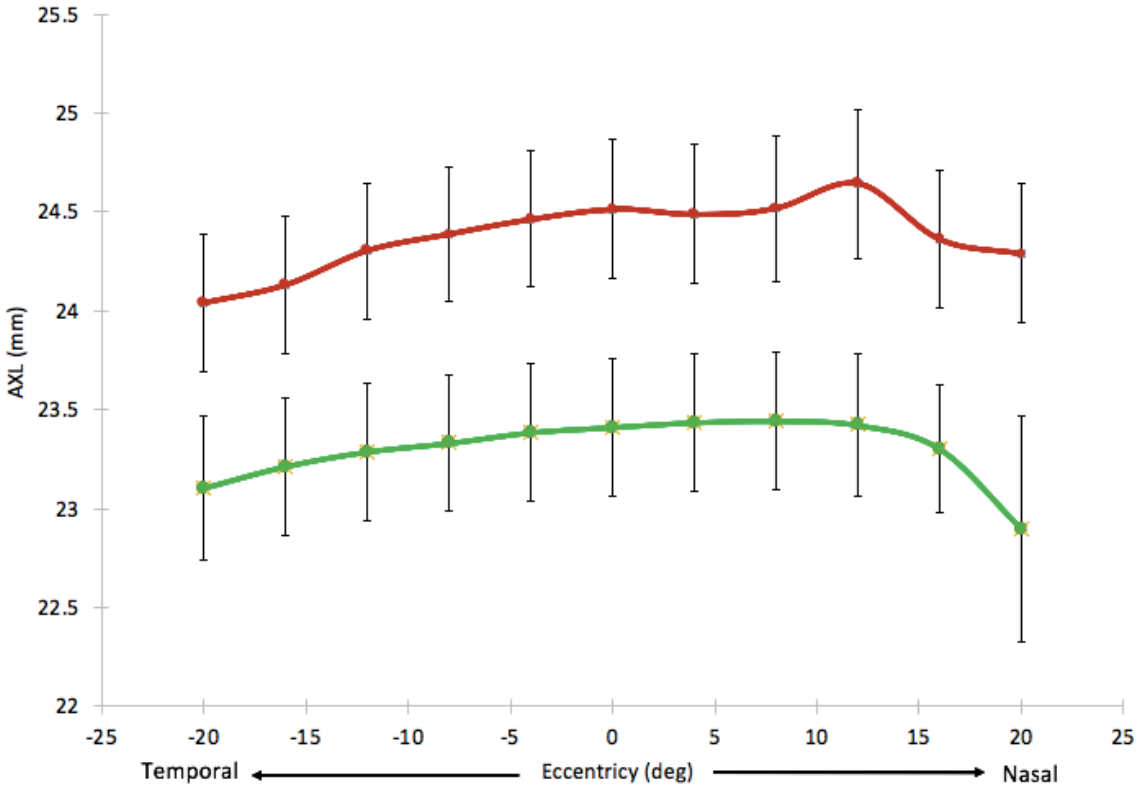


Figure 3.2. Raw AXL values in mm at each eccentricity tested along the horizontal meridian in myopic (red) and emmetropic (green) eyes from temporal (left side) to nasal (right side). Error bars are represented by 95% Confidence Interval.

3.3.2. Conic Fittings

Each subject's retinal shape was fit to a conic function. Accurate (defined as goodness of fit $r^2 > 70\%$) biometric fittings were achieved for most subjects (n=28 of the total n=33 subjects

analyzed). Conic fittings of the horizontal AXL results were described in two facets: asphericity (Q) and apical radius of curvature (C), defined earlier (page 21).

The average Q value for the myopic eyes in our study was -2.0191±0.618, with -1.1939±0.399 for the emmetropic eyes. ANOVA analysis showed significant differences in asphericity between the emmetropic and myopic groups in this study (Welch statistic 10.323, F=18.063, p=0.005); myopic eyes display a more prolate shape than emmetropic eyes. Linear regression analyses showed that AXL approached a significant correlation for asphericity (Pearson R=-0.348, p=0.069) for all eyes; there is a trend for longer AXLs to reveal a more prolate, less oblate retinal shape. Using a two-way ANOVA we found there is no effect of asphericity on race and refractive group (F=0.372, p=0.548) (Figure 3.3).

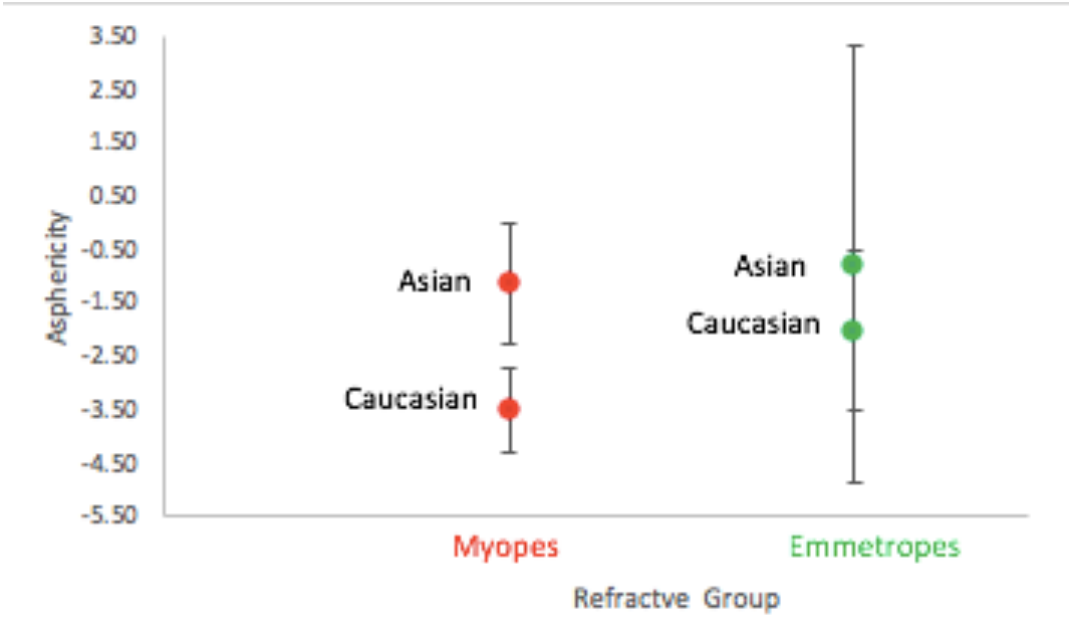


Figure 3.3. Asphericity values for subjects who identified as Caucasian or Asian subjects separated by refractive group with 95% Confidence Intervals

While refractive error and AXL did reveal differences in asphericity, the same cannot be said for the curvature of our subjects. The average C, the vertex radius of curvature of the shape,

for the emmetropic eyes in our study was -0.087±0.003, and -0.090±0.005 for the myopic eyes. The vertex of curvature was minutely smaller but obviously well outside of clinical significance for myopes than emmetropes, as previously reported(81). ANOVA showed no effect of refractive group on curvature (Welch statistic 0.324, F=25.509, p=0.574). Similarly, linear regression analyses showed no correlation of AXL with curvature (Pearson R=0.097, p=0.624).

3.4. Discussion

This study reported AXL values across the central 40 degrees of the horizontal meridian in eyes with emmetropia and myopia. The on-axis AXL for myopic (24.54±0.76 mm) and emmetropic (23.41±0.60 mm) eyes in our study were within the range of those previously reported in healthy adults(70,71,73,82). There was also a strong correlation between on-axis AXL and central refractive error, as expected(70,82,84).

For the group of subjects in this study, peripheral AXLs were shorter than central AXLs, more so for greater eccentricities. Specifically for the group of emmetropes alone, this finding was a trend with no statistical significance, in accordance with previous studies (67,84). On the other hand, there was a significant interaction between eccentricity and AXL in myopic eyes. AXLs became shorter with greater degrees of peripheral eccentricity, creating a more curved myopic profile. It is known that myopic eyes are steeper than emmetropic eyes and the steepness increases with the amount of myopia(50,84,85). Therefore, peripheral AXLs become shorter with eccentricity to a lesser extent in emmetropic eyes compared to myopic eyes. In this study, the pattern was apparent in myopes as early as 4 degrees into the peripheral retina, a finding corroborated by Clark et al(68) who used SD-OCT rather than the PCI method to determine eye shape. The raw AXL data for most subjects could be described as quadratic curves, similar to

previous findings(70), indicating that AXL changes at a greater rate with increased eccentricity. This finding holds true regardless of refractive group. In Schmid et al(77), emmetropic children were followed over a 30 month period. As expected, some children progressed into myopia in that time period. Those children who progressed to myopia in that time showed steeper retinal contours at baseline supporting the hypothesis that eye shape influences the visually guided process of axial eye growth. We argue the study of eye shape in myopic eyes is thus essential to understanding myopic progression, development, and control. On the other hand, a different longitudinal study(84) with already myopic children found that peripheral eye growth was symmetric over a three-year period. The subjects had a steeper temporal retina contour at baseline. In this case, the authors argue that peripheral optical signals may not be a strong stimulus for local growth responses. However, I will say that measurements were only taken at larger angles and the near periphery was not evaluated(84).

Further detail identifies a difference by meridian. The curved profiles were greater temporally than nasally. Tempo-nasal asymmetry along the horizontal meridian with greatest steepening temporally in myopes has been previously reported(68,76,83,84). It should be noted that one previous study found meridional asymmetry only in Caucasian subjects, not in East Asian subjects(87). Attempts were made to include as diverse a population as was possible within the available subject pool. The majority of the subjects in our study were Caucasian. The asymmetry along the horizontal meridian in our study suggests retinal differences in myopic growth and potentially local retinal mechanisms that account for segregated myopic growth regulation.

Accurate biometric fittings from AXL values were achieved for most subjects (28 of a total of 33 subjects) using the fitting a conic function described by Verkicharla et al(76), PCI

method stage 1 (as described in methods section). For this group of emmetropic and myopic individuals, with low to moderate myopia, there was a significant difference noted in asphericity between the emmetropic and myopic groups when fitted to conic functions, with more negative Q values in myopic eyes, indicating that myopic eyes display more prolate shapes than emmetropic eyes. Previous studies have also found similar findings(8,9), although some without statistical significance(81). In spite of this group difference, the correlation AXL and asphericity only approached significance in our study, perhaps due to the limited range of AXL within our subjects. Unlike asphericity, apical radius of curvature showed no effect of refractive group or AXL. Previous research has found that there is a significant increase in curvature as myopia increases; the central radii of curvature is more negative in myopic compared to emmetropic eyes(70,82). Once again, we hypothesize that this difference in central curvature was not replicated in our study because of the limited range of AXL. Nevertheless, our study reveals that the myopic eyes displayed more prolate shapes than emmetropic eyes as asphericity is more negative. It is generally accepted that as myopia increases the ocular contour becomes more prolate, less oblate as the amount of myopia increases. Such findings are well reproduced by many previous articles regardless of methodology, including those using PCI (70,75,76) and SD-OCT (68) methods. However, one previous study(76) found that significant differences could not be replicated in white subjects ($p=0.30$), but was found in Chinese subjects ($p<0.05$). We did not find this to be the case. While we found a significant effect of Q between refractive groups and a trend among AXLs, we did not find any significant race-related differences. Our results were not biased by race.

These results expand the current knowledge of the ocular shape in emmetropia and various degrees of myopia, with differences between the groups but no specific association based

on the amount of myopia given the limited range of myopia in our study. The findings will help determine the potential role of ocular shape, including temporal and nasal asymmetry in myopic development.

4. Peripheral Optical Quality – Aberrations

4.1 Background

Visual input actively guides ocular elongation and refractive error development. Given extensive evidence provided by numerous studies with animal models(13,53,88), the hypothesis that reduced retinal image quality prevents the eye's growth stop signal and ultimately leads to increased eye elongation is now well established. It is also widely accepted that retinal image quality across the periphery, not only at the fovea, plays a significant role in myopia development. However, it is not yet understood what specific types of aberrations or what specific eccentric areas are important to this process. It is not clear how the on-axis and peripheral retinal image quality signals integrate to produce, if any, a final ocular growth stop signal.

Retinal image quality is directly related to the eye's optical aberrations. Since degraded retinal image quality across the retina plays an important role in myopia development, it is postulated that there is an association of the eye's optical quality and myopia. HOA in general and specifically SA may play a role in the eye's failure of emmetropization.

Several studies have investigated the role of HOAs in myopia. I will first discuss HOAs in the center of the myopic retina. While some research has found higher levels of on-axis HOAs in myopic eyes(90,140,120), others found no difference when compared to emmetropic eyes(91,92). Although not universally observed, the former is the more duplicated and consistent finding. Some studies specifically look into the role of SA alone in myopia. Myopic eyes with longer AXLs are repeatedly found to have more on-axis negative SA values(93–96), with increasing negative SA values found in higher amounts of myopia(92,96,97). On the other hand,

emmetropes with shorter AXLs have more positive on-axis SA values(93–96). A few other studies have found this trend but the difference was not statistical significance(98–100).

Overall, the available evidence is not consistently robust to determine the role of on-axis ocular monochromatic aberrations in the development of myopia. As an introduction, I will discuss two longitudinal studies of young children conducted to identify the change in on-axis aberrations over time and the corresponding relationship with refractive development and progression. The first study to correlate HOA and myopic progression was by Zhang et al(101) in which children with fast-developing myopia (progression rate greater than 0.50D per year) revealed higher levels of HOAs than those with slow-developing myopia. The results from this study suggest that there is a role of higher levels of HOA during childhood in abnormal eye growth. In contrast, Philip et al(90) found the baseline HOAs values were significantly higher in emmetropic children that progressed to myopia than for those who emmetropized successfully over a five year period. However, this was only for certain aberrations: third order RMS and coma. Overall optical quality evaluated as RMS-HOA and VSOTF values were both found to be statistically similar between these two groups in the Philip et al study.

Researchers have also studied the effects of individual Zernike terms on AXL and myopic progression. In Philip et al(90), emmetropic eyes that underwent a myopic change also showed an increase in negative SA, while those that stayed emmetropic showed an increase in positive SA. Thus, the authors postulated that the increase in negative SA is a potential trigger in myopic ocular growth. In support of these findings, Lau et al(102) found that a more positive SA at baseline and at follow ups over a two year study period was associated with slower AXL growth, emmetropia, and a reduced risk of myopic shift. It appears that positive SA may impede excessive ocular growth. It is likely that the differences in SA between the refractive groups are

largely due to differences in the crystalline lens(4,12) rather than corneal. Children's eyes that grow towards myopic shifts show thinner crystalline lenses, potentially due to the stretching of the lens from the axial and equatorial ocular growth, but perhaps also a consequence of the myopization process. A thinner lens means a larger radius of curvature and therefore a more negative SA(90). Negative SA induced during extensive accommodation, is a risk factor for myopia in the setting of peripheral hyperopic shifts(29). Without extensive near work, SA is a less concerning myopic progression risk(29). However, when the eye accommodates negative SA increases as well(90). As such, it is possible that increased negative SA in myopia is related to accommodation. For example, one potential mechanism for the role of SA in myopia was put forth by Thibos et al(103) which postulated that negative SA combined with negative defocus, or positive SA combined with positive defocus leads to low attenuated contrast in the defocused image. When combined with the knowledge that high image contrast helps inhibit eye growth(104,105) and that hyperopic blur (negative defocus, e.g., lag of accommodation) activates accommodation, it can be reasoned that underaccommodating eyes (negative defocus) focusing on a near target (inducing more negative SA) may progress towards excessive myopic eye growth. Thibos et al(103) also pointed that SA is not resolution-limited, like VA, thus defocus cues have the same sign across the retina, arguing the importance of studying SA not just on-axis but throughout the field as we present in this study.

We also postulate the importance of measuring optical quality, i.e., aberrations, across the periphery. Generally, all optical aberrations are larger off-axis than on-axis regardless of refractive grouping. Results comparing optical quality across the periphery in emmetropic and myopic eyes are inconsistent, but most find that myopes have larger HOA off-axis than emmetropes(91,96,106–108). For SA specifically, patterns across the periphery differ by

publication as well. Some studies find that SA changes vary little across the meridian regardless of refractive status up to 40 degrees(96)(109). Other studies find slight changes throughout the periphery(92,107–109). In this case, the change across the periphery is best explained by a quadratic rate of change for SA in myopes and emmetropes(106,110).

While it is widely agreed that degradation of retinal image quality plays an important role in the failure of emmetropization, it is unknown which specific aspects of the degraded image quality and at what retinal loci are important for abnormal ocular growth. Understanding of these specifics is important to develop more successful myopia control, and perhaps myopia. Currently, there are limited studies comparing optical aberrations across refractive groups, AXLs, and eccentricities(75,96) with inconsistent results.

The vast majority of these studies use RMS as the optical quality metric, including asphericity and curvature. However, when the intent is to correlate biometric measures or ocular performance measures with the optical quality of the eye, the Strehl ratio based on the optical transfer function (VSOTF) is preferred. The VSOTF is computed using low and high order aberrations for natural pupils to give an estimate of retinal image quality. VSOTF is a relatively new optical quality metric used as objective assessment of the visual system's performance. Computations with VSOTF correlate well with visual performance determined by a strong linear correlation on letters (VA) lost predicted by introduction of wavefront blur(112,113). VSOTF correlates well with visual performance(113) including VA. Perhaps more important is that it correlates regardless of pupil size. VSOTF takes into account neural contrast sensitivity function. It is contrast-sensitivity-weighted and used for diffraction limited optics. For logistics reasons, we did not consider the Stile Crawford effect(90), which is negligible since we did not use cycloplegia. In addition to not using cycloplegia, we did not consider some confounding factors

including pupil size, accommodation, lid pressure, pseudophakia, chromatic aberrations, micro-fluctuations in accommodation(13,114).

In our study, we use VSOTF as an optical quality metric across the central 50 degrees in both emmetropic and myopic individuals. Using this new metric provides fresh information to the field and more easily facilitates the correlation between biometric ocular parameters and optical image quality. Specific attention was given to HOAs and SA in order to expand on the current knowledge on the role of optical image in myopic development and the role of retinal regions/meridians.

4.2 Methodology

4.2.1 Procedure

Measuring peripheral ocular aberrations poses several challenges related to accuracy and feasibility due to long testing times. To overcome some of these methodological difficulties including accuracy, we used a custom-designed scanning Hartmann-Shack wavefront analyzer to measure optical quality (Figure 4.1.). The device measures optical quality ranging from the Zernike order 2^{nd} to 5^{th} (115). It is a scanning wavefront analyzer implying that the base of the scanner rotates across the horizontal meridian to gather information along up to the 80 degrees of the retina. The scanner has a dense sampling density gather one measurement at every single degree(115). Each measurement is collected in just a few seconds, thus well within the natural tear break up time for comfort and accuracy of data. The instrument's measuring range is ± 9.00D of defocus and 5.00D of astigmatism(115). The first scanning aberrometer was studied and published in 2011 by Jaeken et al(116).

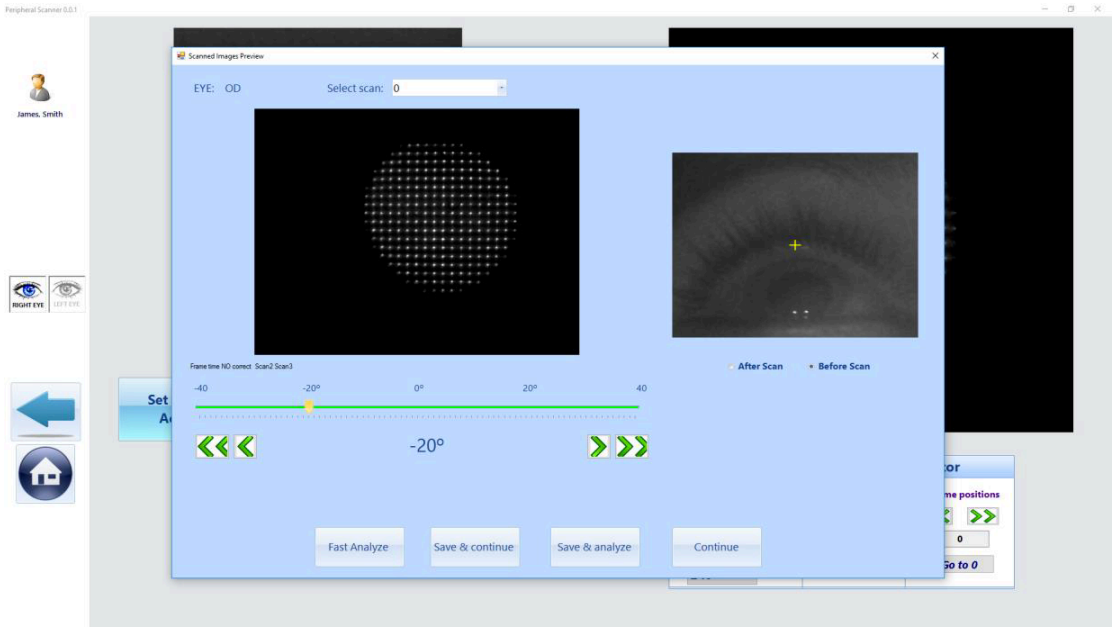


Figure 4.1. View of the screen that appears after each measurement is taken. To the right is the Hartmann-Shack focal spot pattern in the pupil plane. To the left is the iris image to orient the investigator.

The scanning aberrometer keeps the distance between the instrument and the eye equal at all angles(115). A recent study found no differences between this scanning device and other more conventional static devices(117). In the present study, optical quality measurements were analyzed across every point (degree) of the central 60 degrees (30 degrees temporal to 30 degrees nasal to fixation) of the transverse (axial) section. Measurements were taken for five positions of gaze; straight ahead and at four vertical positions. A total of five scanning measurements (with data for 60 eccentricity points) were obtained for each eye: on axis, 8 degrees above and below, 15 degrees above and below the visual axis. Peripheral eccentricities were measured by directing the subject's fixation using a custom designed target (Figure 4.2.). As mentioned previously, it is important to note that 0 degrees (on-axis) was indicated by each

subject's central fixation. This is not necessarily the exact location of the fovea due to angle kappa.

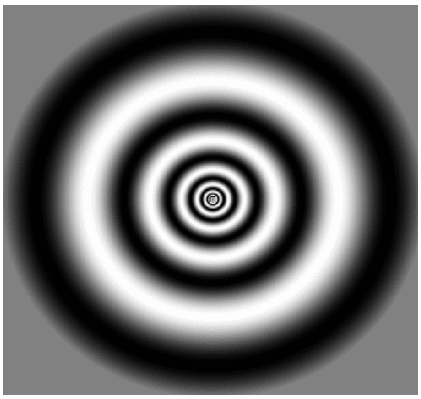


Figure 4.2. Fixation target used during aberration measurements, as described in the text.

Aberration measurements were collected for four different experimental conditions:

a. While the subjects looked without correction at the target located at 4m (for each of the five vertical positions). Data from this section are presented in this Chapter.
b. While the subjects looked with correction, when indicated, at the target located at 4m (for each of the five vertical positions). Data from this section are presented in this Chapter.
c. While the subjects looked with correction at the target located at 50cm (for each of the five vertical positions). Data from this section are not analyzed in this thesis.
d. While the subjects looked straight ahead under complete darkness (tonic accommodation condition). Data from this section are not analyzed in this thesis.

Optical correction was achieved with soft contact lenses that correct each eye within ±0.25D of their best subjective refraction.

4.2.2 Subjects

Three subjects of the 35 were excluded from the optical quality analysis. Just as with the biometry analysis, two subjects were excluded due to their SE refractive error of -0.625D not

meeting the refraction criteria for either Emmetropia or Myopia. For the optical quality analyses, a third subject was removed, this time, due to insufficient raw aberrometry data.

4.2.3 Data Processing and Analyses

The raw aberrations data from the remaining 32 subjects were exported from the aberrometer and imported into Matlab. Only right eye data is presented in this thesis. Also, aberrations data are presented for the horizontal position only. The condition of 4m with correction (myopes) or 4m without correction (emmetropes) was used in this Chapter's analyses. Appendix 1 details a full account of all on-axis optical quality metrics collected for the right eye of all subjects at the horizontal meridian.

Eccentricity (degrees)	Location	Range degrees averaged	Location
-25	Temporal	-27 to -23	Temporal
-20	Temporal	-22 to -18	Temporal
-15	Temporal	-18 to -13	Temporal
-10	Temporal	-12 to -8	Temporal
-5	Temporal	-7 to -3	Temporal
0	Temporal/Nasal	-2 to +2	Temporal/Nasal
5	Nasal	+3 to +7	Nasal
10	Nasal	+8 to +12	Nasal
15	Nasal	+13 to +17	Nasal
20	Nasal	+18 to +22	Nasal
25	Nasal	+23 to +27	Nasal

Table 4.1. Optical quality data was collected at every degree along the horizontal meridian. In our analysis, we grouped together every five degrees. It is important to note that 0 degrees is defined with a central fixation target, thus it is not necessarily the exact location of the fovea because of angle kappa. See eccentricity legend.

Raw data were collected at each degree along the horizontal meridian and VSOTF values calculated for each degree. To compute optical quality metrics, we considered either VSOTF or

RMS (root mean squared). Both standard metrics used in the studies of ocular aberrations. While RMS is more common, for the reasons explained above, VSOTF is preferable to show optical quality. For statistical analysis purposes, VSOTF data were grouped by five degree increments to form eccentricity groupings. There were a total of eleven eccentricity groups used in the statistical analyses (Table 4.1.).

Using SPSS, a mixed (between/within) model of variance was used to evaluate the relationship between eccentricity and refractive group. Because the sphericity assumption was violated, $\chi 2$ (54) = 302.142, $p<0.001$, the Huynh-Feldt correction was used in the results below.

4.3 Results

Analyses showed an overall effect of eccentricity ($F=11.057$, $p<0.001$, $\eta_p^2=0.269$) and a main significant interaction between eccentricity and refractive group ($F=2.257$, $p=0.049$, $\eta_p^2=0.070$), with myopic eyes showing more negative VSOTF values temporally (Figure 4.3.). Within-subject contrast testing revealed eccentricity was best explained with a quadratic fit ($F=32.989$, $p<0.001$, $\eta_p^2 =0.524$) with VSOTF decreasing at a higher rate temporally than nasally for all subjects (Figure 4.3), similarly to what was observed for off-axis AXL in myopic eyes in Chapter 3.

To demonstrate the different behavior of VSOTF temporally between myopic and emmetropic eyes, individual one-way ANOVAs were computed. Emmetropic eyes have more positive VSOTF than myopic eyes for the 25 ($F=5.125$, $p=0.031$), 20 ($F=5.665$, $p=0.024$) and 15 ($F=5.560$, $p=0.025$) degree eccentricities temporally, and approached significant differences at 5 degree temporally ($F=3.325$, $p=0.078$).

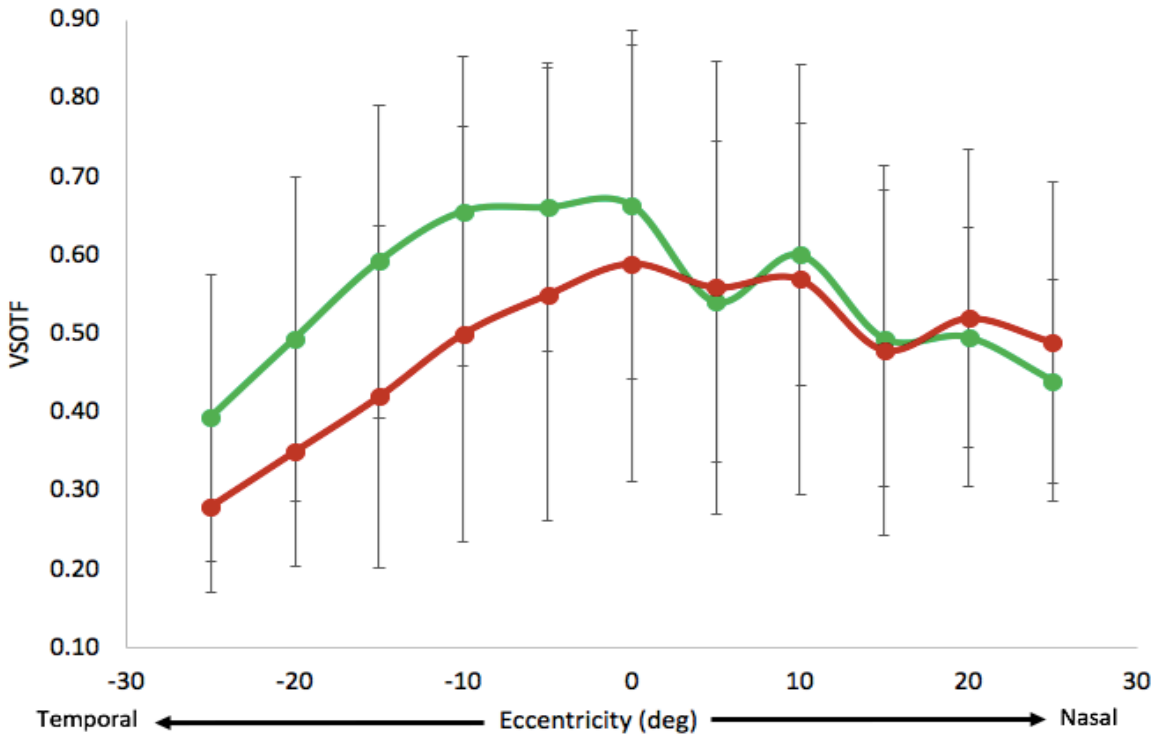


Figure 4.3. VSOTF values in microns at each eccentricity tested along the horizontal meridian in emmetropic (green) and myopic (red) eyes. Error bars are represented by 95% Confidence Intervals.

4.3.1 Overall Optical Quality

Analyses were performed for each refractive group separately to evaluate the effect of eccentricity in refractive error. Because the Sphericity assumption was violated, $\chi 2$ (54) = 229.123, $p<0.001$, the Huynh-Feldt correction was used. An overall effect of eccentricity ($F=8.897$, $p<0.001$, $\eta_p^2=0.319$) was found in myopic eyes. Within-subject contrast testing revealed peripheral optical quality was equally explained with quadratic ($F=16.416$, $p=0.001$, $\eta_p^2 =0.464$) and linear ($F=16.277$, $p=0.001$, $\eta_p^2 =0.461$) fits.

Pairwise comparisons showed differences among all peripheral eccentricities including between 15 degrees temporal and 15 degrees nasal and most points compared to 20 and 25 degrees nasal. In general, temporal eccentricities show more negative VSOTF indicating worse optical quality in adult myopes.

The Sphericity assumption was also violated for emmetropic eyes' data, $\chi 2$ (54) = 139.921, $p<0.001$, and the Huynh-Feldt correction was used. An overall effect of eccentricity ($F=5.538$, $p=0.001$, $\eta_p^2=0.335$) was also found in emmetropic eyes. Within-subject contrast testing revealed peripheral optical quality was equally explained with quadratic ($F=19.779$, $p=0.001$, $\eta_p^2 =0.643$) and cubic ($F=14.792$, $p=0.003$, $\eta_p^2 =0.574$) fits, indicating somewhat a similar shape of the VSOTF across the periphery in emmetropic and myopic eyes. Both emmetropes and myopes took on quadratic shapes however, emmetropes also followed a cubic fit while myopes followed a linear fit.

Pairwise comparisons showed differences only between at a few eccentricities, such as between 20 degrees temporal and 15 degrees temporal and on-axis (0 degrees), and between 5 degrees nasal and 10 degrees nasal. There were no differences between nasal and temporal periphery in adult emmetropes, unlike those noted in myopes.

4.3.2 Spherical Aberration

In agreement with previous findings, myopes showed more negative SA and emmetropes showed more positive SA values in our study (Figure 4.5). Because the Sphericity assumption was violated, $\chi 2$ (54) = 214.336, $p<0.001$, the Huynh-Feldt correction was used. A mixed model analysis of variance showed an overall effect of eccentricity ($F=3.765$, $p=0.003$, $\eta_p^2=0.112$), with a trend towards higher SA values for temporal than nasal eccentricities. However, no main significant interaction between eccentricity and refractive group ($F=1.243$, $p=0.292$, $\eta_p^2=0.040$) was noted. When all subjects were analyzed together, 95% of cases were explained by a linear fit ($F=13.606$, $p=0.001$, $\eta_p^2 =0.312$).

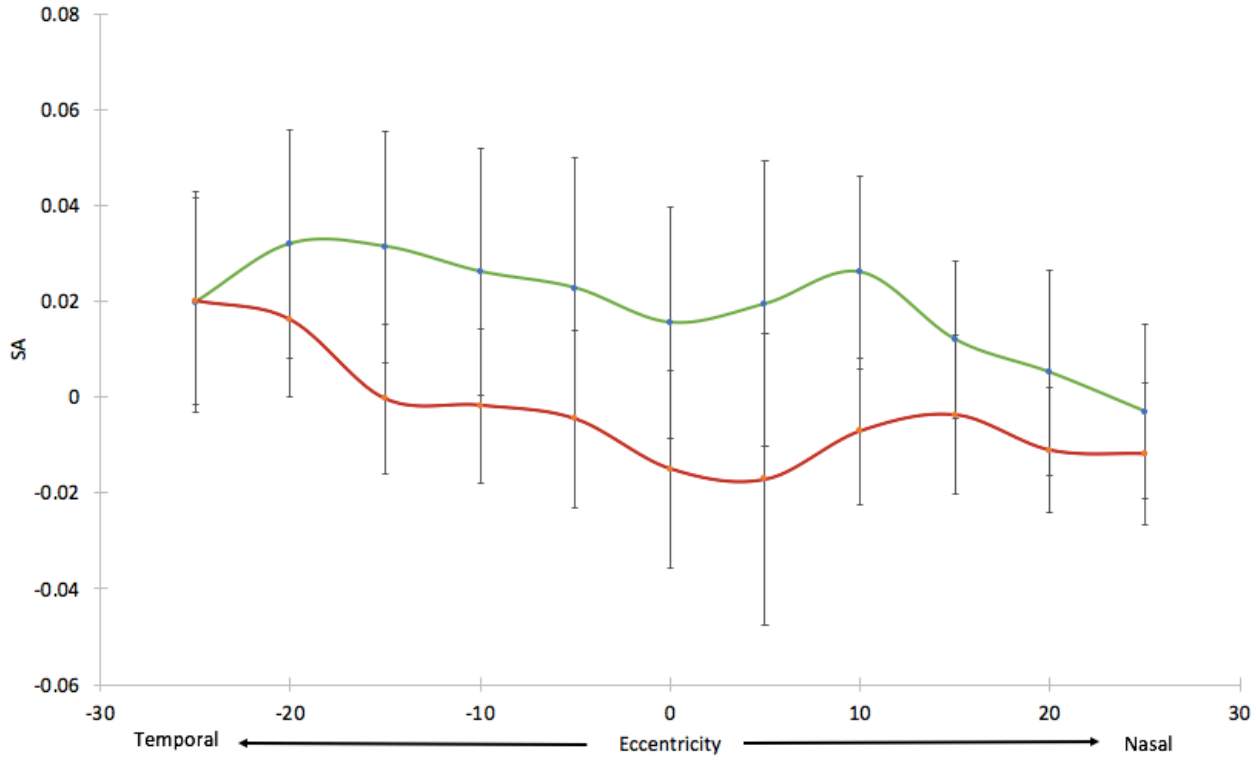


Figure 4.5. SA values in microns at each eccentricity tested along the horizontal meridian in emmetropic (green) and myopic (red) eyes. Error bars are represented by 95% Confidence Intervals.

Individual one-way ANOVAs showed emmetropes have larger, more positive SA for the more central values, specifically, significant differences were found at 15 degrees (F=4.909, p=0.034), 10 degrees (F=4.323, p=0.046), and 5 degrees (F=3.346, p=0.077) temporally, on-axis (F=4.398, p=0.045), and at 10 degrees nasally (F=7.939, p=0.008).

When myopic eyes were analyzed separately, a significant overall effect of eccentricity on SA was found (F=2.897, p=0.002, η_p^2=0.132). Peripheral SA values in myopes were best explained by a linear fit for 80% of subjects (F=8.626, p=0.008, η_p^2 =0.312). For emmetropic eyes, the effect of eccentricity on SA was also significant (F=3.390, p=0.005, η_p^2=0.236). Peripheral SA values in emmetropes were best explained by a linear fit for 65% of subjects (F=6.629, p=0.026, η_p^2 =0.376).

4.4 Discussion

Using a novel scanning aberrometer we collected a large amount of optical quality data across 50 degrees of the field in a group of emmetropic and myopic eyes. From the optical wavefront aberrations obtained at each eccentricity, every 1 degree, VSOTF values were computed. Data were obtained for 12 emmetropic and 20 myopic adults, providing us with the ability to identify optical image quality properties across the periphery in myopia. Subjects were homogenous in age and other factors allowing for a reduced number of confounding factors. Only the horizontal meridian results for the right eye are reported here, however we have data along the vertical data constituting a 50x30 2D map of retinal image quality which will be prepared for publication. In terms of limitations, there is a limited range in AXL for our myopes as most of our myopic refractive errors were mild or moderate. Specific to this instrument, we used contact lenses to attain optical correction for our myopes. Finally, we did not consider chromatic aberrations for this thesis.

Variability in optical quality across the periphery was found between subjects, similarly to previous studies(118,119). Interindividual variability in the optical shape of the eye may be due to pre-determined optics in childhood, although a previous study showed that intersubject variability is greater in adults as compared to children(1,3). Our study showed greater standard deviation errors for myopic than emmetropic eyes, indicating greater interindividual variability in myopes.

In our study, we found an overall effect of VSOTF as a function of eccentricity for all subjects and by refractive group. Myopic eyes in general showed more negative VSOTF values, indicating worse optical quality than emmetropic eyes. Previous research have inconsistencies,

though the trend points to an overall poorer myopic optical quality across the horizontal meridian (peripheral 40 degrees) compared to other refractive errors (114,120), as we found.

VSOTF values were more positive (better optical quality) nasally than temporally in emmetropic but not myopic eyes. When emmetropic and myopic eyes were compared, myopes showed more negative (worse optical quality) VSOTF temporally at all peripheral eccentricities, revealing a trend to significance as early as 5 degrees from the on-axis values. In a previous study(120), HOAs did not vary across the periphery (defined as the central 40 degrees) by refractive group arguing against the common hypothesis that peripheral blur serves as a cue for excessive ocular growth. However, the authors did find HOAs varied by eccentricity. Specifically, RMS-computed HOAs were greater nasally than temporally in all subjects, similar to our findings. Another study found larger RMS-computed HOAs temporally than nasally(111), also similar to our findings. This implicates some amount of repeatability of our data even when using a different optical quality metric. The main difference between these studies was age and thus potentially accommodative response abilities although the younger subjects underwent cycloplegia, partially negating this concern. A contradictory study with the similar method of relying on a scanning aberrometer to find that HOA across the periphery(114), found that second-order and third-order RMS showed a strong variation in eccentricity with higher values temporally compared to nasally, similar to our findings. The largest difference between emmetropes and myopes was found at the nasal retina. Although this finding conflicts with ours, their observation in variation was very small(114).

In our study, the effect of eccentricity in optical quality was best explained with a quadratic fit with VSOTF decreasing at a higher rate temporally than nasally for all subjects. For over half of the emmetropic and the myopic eyes, optical quality was best explained with

quadratic fits, but the remaining eyes in both were different, indicating that the shape of VSOTF across the periphery is partially consistent across refractive groupings. Interestingly, as previously explained in Chapter 3, the raw AXL data for most subjects were also best described as quadratic curves. Thus it is important to note that we found overlap when comparing ocular shape measured with biometry and ocular shape measured with optical quality. When reviewing results of previous studies evaluating aberrations across the periphery, inconsistencies were identified in the literature. Some previous studies found a quadratic shape in ocular aberrations across the horizontal periphery(23), while, others found no trend of aberrations across eccentricities.

In this study, we also specifically observed the effect of eccentricity and refractive grouping on SA. As expected(90,96,102,109), we found more positive SA values in emmetropes and more negative SA values in myopes. This finding was most prominent centrally, although it also held true for the majority of subjects in the periphery. Additionally, SA was greater in myopes compared to emmetropes and larger amounts of SA were found in higher amounts of myopia. This is well documented throughout the literature(92,96,97). What is less studied is how SA changes throughout the periphery. Some studies find that SA changes vary little across the measured meridians(96). Other studies find changes throughout the periphery(106,110). In our study, we found a trend of asymmetry comparing either side of horizontal meridian. While almost all subjects showed peripheral SA values that were best explained with a linear fit, there was a trend towards higher SA values for temporal than nasal eccentricities. Emmetropes had larger, more positive SAs centrally than peripherally, and the opposite was true for myopes. There is very limited previous data on the shape of SA across the periphery, but some previous

studies have found that the change in SA across the periphery follows quadratic changes(106,110).

Reduced image quality across the periphery remains even when central refractive error is corrected for due to the strong presence of HOAs and SA. This study was done in young adults with stable refractive errors and the myopic subjects had only low and moderate amounts of myopia. As explained in detail earlier in the thesis, some research points to the role of higher levels of HOA during childhood in faster myopic eye growth(101), while others observe no difference in retinal image quality comparing baseline to development/progression of myopia(90). At this time point, more work is needed to provide conclusive evidence indicating that HOAs play a role in the development of myopia.

These results expand our current knowledge of optical image quality across the horizontal periphery in emmetropia and various degrees of myopia in addition to identifying the differences between nasal and temporal meridians. In sum, these findings will help provide further context for the role of peripheral optical image quality in myopia and refractive error development.

5. Comparison of Peripheral Biometry and Optical Quality Contours

5.1 Background

Degraded retinal image quality is thought to provide abnormal feedback during a child's normal eye growth control, disrupting emmetropization, and leading to excessive myopic growth. Important factors in determining the retinal image quality are the optical quality of the eye, ocular aberrations, and the shape of the eye, ocular biometry. Aberrations and ocular biometric parameter changes are both age-related(73,74) and specific to refractive error(122). There is a question of whether optics influences myopic development or progression through (for example) eye or retinal shape. And vise versa. Structural changes in the eye associated with refractive errors alter not just the axial aberrations but also the peripheral aberrations of the eye. Significant differences in aberrations by refractive groups may occur as a consequence of biometry changes. Because our study find significant associations between refraction and HOA we wonder if HOA is playing a role in trigger or progressing myopic change. And so, we argue that in addition to measuring AXL, perhaps aberrations should be considered into models of myopia development and progression.

The study of optical quality metrics must be supplemented with the study of biometric parameters as significant changes in optical quality and differences in aberrations between refractive groups can be attributed to biometric parameters differences. Thus, changes in HOA or SA can occur as a consequence of changes to biometric characteristics in lens or eye length. For example, the myopic eye grows following an axial expansion of the eye, as a consequence the lens undergoes radial stretching contributing to the thinning and flattening of the lens in myopes more so than in emmetropes. These biometric changes play a significant role in SA in myopes leading to a higher amount of negative SA(122).

Previous literature has drawn oversimplifications between eye shape, retinal shape, and peripheral refraction. For example, while related, refractive pattern alone is not sufficient information to correctly identify eye shape, and more so, eye shape must not be confused with retinal shape. Eye shape must also take into account the anterior structures of the eye thus an AXL measurement, corneal curvature, and the crystalline lens should all be studied together rather than retinal shape alone. Equally important, the eye's optics must also be considered(70).

In this final chapter, we studied the role of optical and biometric properties in determining the eye shape in adult myopic and emmetropic eyes. Specifically, we investigated the role of individual optical quality, measured as HOAs (VSOTF) and SA. As explained throughout this paper, many authors have produced work comparing optical characteristics and/or biometric characteristics between refractive errors in adults and children, or between isomyopes and anisomyopes(123). For example, Tian et al(92) studied the optical quality of isomyopes and anisomyopes and separately analyzed the ocular parameters and refractive profiles of these subjects. The myopic subjects had more prolate asphericity and a more positive SA profile across the periphery, as expected and similar to our study(92). There was a negative correlation between peripheral SA and central myopia, however, unlike our study, there was not a statistically significant correlation between HOA across the periphery and myopia(92). However to our knowledge, this thesis is the only study that has done a direct comparison of both the biometric and optical properties across the periphery in emmetropic and myopic eyes. In this final part of the study we present a comparison of the biometric properties (AXL) and optical aberrations (VSTOF and SA) in our group of emmetropes and myopes.

5.2 Methodology

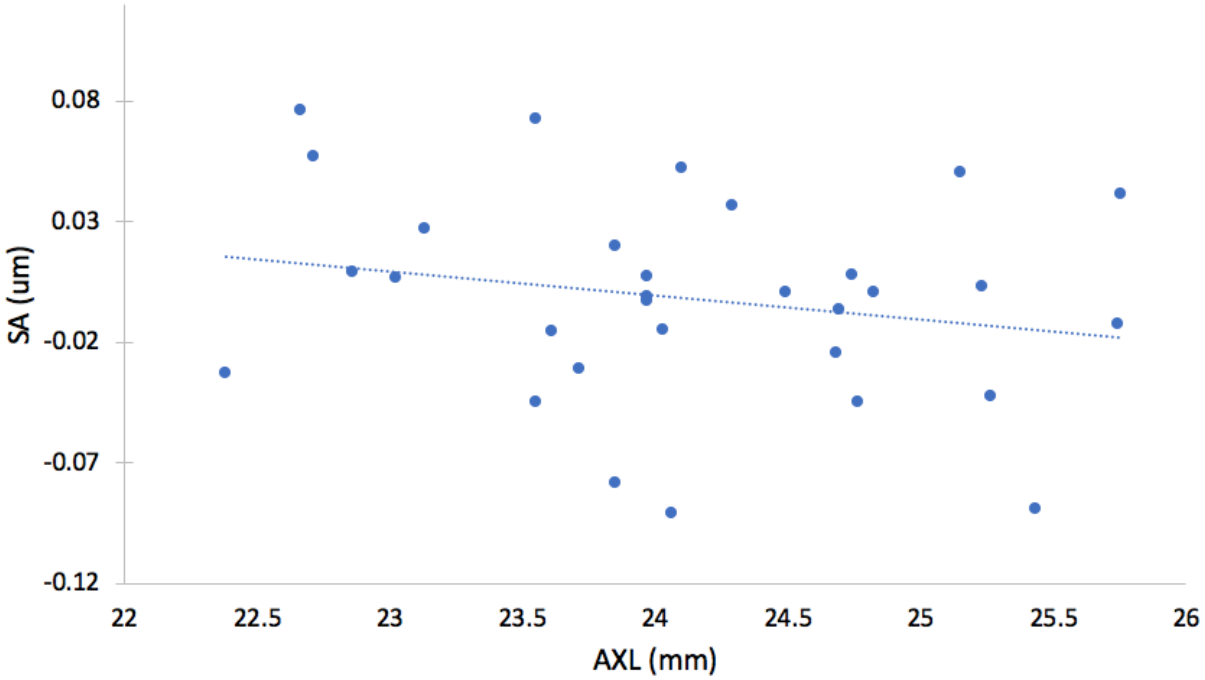
Central and peripheral eye length was obtained using the Lenstar partial coherence interferometer as explained in Chapter 3. Central and peripheral retinal image quality was computed using VSOTF metrics, as explained in Chapter 4. These two parameters were correlated with linear regression using SPSS.

Because two different metrics were compared, we had two limitations in these analyses. First, while VSOTF data were computed at every degrees along the horizontal meridian, AXL data were only collected at 11 specific points, as such all statistical comparisons were limited to those specific eccentricities. Thus, 11 points within the central 40 degrees of the transverse (axial) section were studied: 20 degrees, 16 degrees, 12 degrees, 8 degrees, 4 degrees, on-axis (0 degrees). Second, while we had biometry data from 33 subjects, we only had optical quality data from 32 subjects; thus we only used the data from 32 subjects. As with previous chapters, only the right eye data is presented.

5.3 Results

Linear regression analysis revealed no correlation between on-axis AXL and on-axis optical image quality metric VSOTF (Myopes: Pearson R=-0.150, p=0.541; Emmetropes: Pearson R=-0.247, p=0.439). However, for all subjects and across the entire horizontal meridian, results revealed that overall shorter peripheral AXL values are correlated with more negative VSOTF (poorer optical quality) (Pearson R=-0.111, p=0.042). While this result is statistically significant, the correlation remained small. This is likely because the correlation was not consistent for all subjects. Specifically, half the myopic eyes (n=10 of a total of n=20 subjects) showed a significant correlation between AXL and VSOTF across the central 40 degrees. While

the majority of these subjects showed a positive correlation, three of them revealed a negative correlation. For emmetropes, only one-third (n=4 of a total of n=12 subjects) showed a significant correlation between AXL and VSOTF. Of these four subjects, half were positive correlations and have were negative. For both emmetropes and myopes, no significant association was found between those subjects with significant correlation AXL/VSOTF and the ratio AXL/RE.



5.1. Correlation between on-axis AXL and on-axis SA across the central 40 degrees for all subjects tested.

Linear regression analyses also revealed no significant correlation between on-axis AXL and on-axis SA (Myopes: Pearson R=-0.134, p=0.585; Emmetropes: Pearson R=-0.358, p=0.253), see Figure 5.1. However, across the horizontal meridian, results revealed an overall significant negative correlation between SA across eccentricities and on-axis AXL (Pearson R=-0.195, p<0.001), with more negative SA in longer AXL. Although significant, this correlation is

also small. Specifically, one-third (n=7 of a total of n=20 subjects) showed a significant correlation between AXL and VSOTF across the central 40 degrees. The vast majority of these (n=6) showed a negative correlation and only one revealed a positive correlation. For emmetropes, a similar percentage (n=5 of a total of n=12 subjects) showed a significant correlation between AXL and VSOTF across the central 40 degrees. In contrast to the findings in the myopic subjects, these 5 emmetropic subjects showed positive correlations, with more positive SA with longer AXL. Thus the effect of more negative SA in longer AXL is only in myopia. For both emmetropes and myopes, no significant association was found between those subjects with significant correlation AXL/SA and the ratio AXL/RE.

5.4 Discussion

While there is no correlation on-axis between AXL and VSOTF, peripheral AXL is directly correlated with VSOTF values, meaning that eyes with overall shorter peripheral AXL values are correlated with more negative VSOTF (poorer optical quality). This further confirms that myopic retinal contours are steeper than emmetropic eyes, and continue to steepen with increased amounts of myopia. Previous research has shown inconsistent results, though the trend points to an overall poorer myopic optical quality across the horizontal meridian (peripheral 40 degrees) of eyes with shorter peripheral eye lengths relative to central (114,120). We observed the greatest amount of inter-subject variability when correlating retinal profile and image focus than when studying either metric alone.

In this study we also found a negative correlation between on-axis AXL and peripheral SA values. Although the correlation was small, a more negative peripheral SA is more likely to be found in a longer eye (longer on-axis AXL). As expected(90,96,102,109), we found more

positive SA values in emmetropes and more negative SA values in myopes. Longer on-axis AXLs are repeatedly found to have more on-axis negative SA values(93–96), with increasing negative SA values found in higher amounts of myopia(92,96,97). As previously explained in Chapter 4, longitudinal studies with young children have found that emmetropic eyes that undergo a myopic shift have an increase in negative on-axis SA(90); also a more positive SA at baseline and follow ups may be associated with a reduced risk of myopia(102). It appears possible that the amount and sign of SA may trigger or impede excessive ocular growth. As previously explained in Chapter 4, the effect of the periphery on SA is still underdeveloped in the literature. In this study we found peripheral SA is best fit with a linear function while others(106,110) have found that SA changes across the periphery best fit a quadratic function. This method gives relatively accurate retinal shape results(70). Accurate measures of AXL and retinal shape are considered essential diagnostic and treatment tools for myopia. The PCI approach provides a cheaper, faster, and less cumbersome option than the MRI. In this study, we compared the optical and biometric characteristics of emmetropic and myopic eyes across the horizontal periphery to determine how eye shape and image quality play a role in myopic development.

6. General Conclusions

Understanding peripheral retinal controls is essential to the development of emmetropization models. It is known that the degradation of retinal image quality across the periphery leads to excessive myopic eye growth. This study presents biometry (AXL) and optical quality (VSOTF and SA) measurements, as well as a novel comparison between these, across the central 50 degrees in eyes with emmetropia and various degrees of myopia.

This thesis shows the influence of refractive error and meridian on eye shape with AXL as the primary metric. Chapter 3 explains how myopes have steeper retinal contours than emmetropes, with the steepening significantly increasing along the horizontal meridian as on-axis myopia increases. A similar pattern is found for asphericity, with a more prolate, or less oblate, peripheral contour in myopes compared to emmetropes. On the other hand, the apical radius of curvature does not significantly vary with AXL or refractive group. Myopes and emmetropes biometric shapes follow a quadratic conic fit that reveal naso-temporal asymmetries with increased temporal curvature starting as early as 4 degrees temporal and extending all the way out to 30 degrees temporal. It is well established that myopic contours are more curved, however where that significance begins is not always recorded. Our results further emphasize the potential role of the near periphery in retinal contour differences between refractive groups and therefore in emmetropization modeling. It was already known that retinal shape changes in myopia, however it is not yet known whether eye shape influences the visually guided process of axial eye growth and thus is a driving factor for myopia development or it is merely a consequence of such growth(70,81). Retinal steepness across the periphery could potentially be a risk factor for myopia development(77). We argue that the naso-temporal asymmetry between meridians points to the potential presence of local retinal mechanisms that account for segregated

myopic growth regulation further, corroborated by the presence of this asymmetry in emmetropic children prior to the development of myopia(77). This supports the hypothesis that eye shape influences the visually guided process of axial eye growth, influencing our desire to further explore the retinal shape in myopic eyes.

Secondly, this thesis presents image quality data, for all HOA and also for specifically SA, across the entire horizontal meridian. Chapter 4 results reveal that myopic eyes have overall worse optical image quality across the peripheral horizontal meridian than emmetropic eyes, once on-axis refractive errors are corrected. Peripheral optical shapes are also best explained with quadratic fits, with the temporal retina showing the largest difference in HOA between emmetropes and myopes revealing a trend to significance as early as 5 degrees from the on-axis values. Specifically when studying SA, myopes have a more negative SA value than emmetropes across the periphery although this modest difference is less prominent as eccentricity increases. SA shapes across the horizontal meridians are best explained with linear fits, but with a trend towards higher SA values for temporal than nasal eccentricities. It is argued that peripheral blur may serve as a trigger for myopia development(101,102). Near peripheral optical quality is thought to play a role in the failure of emmetropization and thus serve as a target for myopia control methods(116).

With peripheral ocular shape and retinal image quality possibly playing a large role in myopia development and progression, it is timely that we investigate how eye shape, determined by biometry, and image quality, determined by ocular aberrations, are associated. The final part of this thesis found correlated biometric parameters with optical image quality across the periphery of myopic and emmetropic eyes. There was no correlation on-axis between AXL and VSOTF, but peripheral AXL is directly correlated with VSOTF values, meaning overall shorter

peripheral AXL values are correlated with more negative VSOTF (poorer optical quality). Additionally, there was a negative correlation on-axis between AXL and peripheral SA, with a more negative peripheral SA in longer eyes (axial AXL). SA may play a role in emmetropization as the increase in on-axis negative SA is a potential trigger in myopic ocular growth studies(90) and it is possible that on-axis positive SA may impede excessive ocular growth(102). The role of peripheral SA in emmetropization in children is yet to be elucidated.

This study is innovative because we conducted a combined study of both geometric and optical metrics in the setting of retinal contour across the peripheral retina. It is generally agreed that degraded retinal image quality plays a role in the failure of emmetropization; because aberrations quantify degraded image quality, there is potential to link increased aberrations with myopic progression. Thus, in addition to measuring AXL, aberrations should be incorporated into models of myopia treatment and prevention. Further studies will be necessary to construct a full optical model of individualized 3D eye models using biometry, corneal curvature, the lens, refraction, and optical image quality in a central and peripheral matrix. Additionally, image quality should be studied in conjuncture with vision sensitivity across the retina in a monocular and binocular context.

7. Appendix 1

On-axis raw aberration values for each subject: sphere, cylinder, axis, M, J0, J45, RMS-HOA, Z12, coma:

	Sphere	Cylinder	Axis	M	J0	J45	RMS-HOA	Z12	COMA
PBM001	-0.3172	-0.3522	5.0000	-0.4933	0.1728	0.0333	0.1445	0.0648	0.0128
PBM002									
PBM003	-0.3104	-0.4449	151.0000	-0.5328	0.1137	-0.1909	0.1622	0.0672	0.0235
PBM004	-0.1853	-0.1316	163.0000	-0.2511	0.0549	-0.0358	0.1807	0.0185	0.1024
PBM005	-0.4404	-0.6129	167.0000	-0.7468	0.2762	-0.1327	0.1257	0.0567	0.0071
PBM006	0.0413	-0.2336	165.0000	-0.0756	0.0998	-0.0608	0.1225	-0.0849	-0.0118
PBM007	0.2271	-0.6187	87.0000	-0.0822	-0.3078	0.0289	0.2617	0.0833	0.0039
PBM008	-2.6289	-0.7515	165.0000	-3.0046	0.3249	-0.1885	0.1204	0.0024	0.0918
PBM009	0.2481	-0.3521	159.0000	0.0721	0.1308	-0.1178	0.2007	-0.0937	0.0464
PBM010	0.5746	-0.1730	171.0000	-0.2906	0.6504	0.5704	0.4487	-0.0627	-0.0233
PBM011	0.5071	-0.3439		0.3351	0.1723	0.0013	0.1399	-0.0042	0.0514
PBM012									
PBM013	0.1193	-0.3198	71	-0.0406	-0.1266	0.1005	0.1863	-0.0376	0.0694
PBM014									
PBM015	-0.6122	-0.4587	146	-0.8415	0.0872	-0.2122	0.1557	-0.0215	0.0671
PBM016									
PBM017	-0.6931	-0.6561	175	-1.0212	0.3224	-0.0604	0.1306	-0.0060	0.0224
PBM018									
PBM019	-1.1695	-0.4157	74	-1.3774	-0.1775	0.1089	0.1127	-0.0191	-0.0586
PBM020	0.6286	-0.9958	70	0.1308	-0.3805	0.3209	0.2297	-0.0520	0.0590
PBM021	-0.3912	-0.0432	32	-0.4127	0.0095	0.0194	0.1732	-0.0144	-0.0274
PBM022	-0.3003	-0.4834	112	-0.5420	-0.1716	-0.1703	0.1645	-0.0434	0.0100
PBM023	-0.7604	-0.7106	109	-1.1157	-0.2767	-0.2232	0.1655	0.0043	-0.0715
PBM024	-0.8781	-0.5210	133	-1.1386	-0.0183	-0.2599	0.1387	0.0530	0.0108
PBM025	0	0.3097	-0.2442	143	0.1876	0.0348	-0.1172	0.1510	0.0728
PBM026	0.1093	-0.3462	36.0000	-0.0638	0.0535	0.1646	0.2014	-0.0190	0.0000
PBM027	-0.1776	-0.6746	163.0000	-0.5149	0.2770	-0.1913	0.2402	-0.0218	-0.1219
PBM028									
PBM029	0.1165	-0.2905	95.0000	-0.0287	-0.1432	-0.0239	0.1709	-0.0310	-0.0241
PBM030									
PBM031	0.2141	-0.1343	171.0000	0.1470	0.0640	-0.0197	0.1407	0.0158	0.0686
PBM032									
PBM033	0.1716	-0.9556	2.0000	-0.3062	0.4766	0.0282	0.2126	-0.0107	0.1621
PBM034	-6.9482	-0.7756	9.0000	-7.3360	0.3682	0.1218	0.1050	0.0014	0.0574
PBM035	-1.7827	-0.9876	96.0000	-2.2765	-0.4835	-0.0993	0.1714	0.0054	-0.0115

On-axis raw aberration values for each subject: Z6 to Z20:

	Z6	Z7	Z8	Z9	Z10	Z11	Z12	Z13	Z14	Z15	Z16	Z17	Z18	Z19	Z20
PBM001	-0.0383	0.0783	0.0128	0.0334	-0.0099	-0.0150	0.0648	-0.0358	0.0077	0.0225	0.0290	-0.0299	-0.0058	-0.0122	0.0232
PBM002															
PBM003	-0.1181	-0.0054	0.0235	0.0363	0.0152	0.0041	0.0672	0.0030	0.0543	0.0053	0.0096	-0.0115	0.0025	-0.0168	0.0098
PBM004	-0.0423	0.1297	0.1024	-0.0153	0.0139	-0.0017	0.0185	-0.0275	0.0062	-0.0054	-0.0148	-0.0053	-0.0018	0.0124	-0.0261
PBM005	-0.0906	-0.0027	0.0071	-0.0384	-0.0146	-0.0189	0.0567	0.0063	-0.0018	0.0089	0.0047	-0.0025	0.0032	0.0082	0.0067
PBM006	-0.0264	0.0210	-0.0118	-0.0392	0.0126	0.0029	-0.0849	0.0019	-0.0037	-0.0122	0.0217	-0.0123	-0.0053	0.0163	0.0207
PBM007	-0.1089	0.1750	0.0039	0.0969	0.0023	-0.0072	0.0833	-0.0325	0.0178	-0.0073	-0.0027	0.0156	0.0107	-0.0043	-0.0095
PBM008	-0.0308	0.0297	0.0918	0.0314	0.0262	-0.0050	0.0024	-0.0039	0.0125	0.0033	0.0052	-0.0144	0.0036	0.0032	-0.0019
PBM009	0.0181	-0.0016	0.0464	0.0717	-0.0455	-0.0151	-0.0937	-0.0163	-0.0617	-0.0615	0.0474	0.0525	0.0724	0.0583	
PBM010	0.0568	-0.2767	-0.0233	0.1544	0.1675	-0.1174	-0.0627	-0.0357	-0.0225	0.0394	0.0329	-0.1257	-0.0855	-0.0362	-0.0298
PBM011	-0.0606	-0.0159	0.0514	-0.0083	0.0384	-0.0007	-0.0042	-0.0049	0.0137	0.0121	0.0205	0.0234	-0.0207	0.0270	-0.0112
PBM012															
PBM013	-0.0972	-0.0561	0.0694	0.0438	-0.0190	0.0300	-0.0376	-0.0446	-0.0279	0.0150	0.0159	0.0445	0.0055	0.0181	-0.0192
PBM014															
PBM015	0.0053	0.1254	0.0671	-0.0078	0.0306	-0.0065	-0.0215	-0.0080	0.0150	-0.0029	0.0032	0.0237	0.0145	-0.0084	0.0146
PBM016															
PBM017	-0.0217	0.0472	0.0224	0.0942	-0.0208	0.0107	-0.0060	0.0329	-0.0288	-0.0195	0.0220	0.0038	0.0094	-0.0120	0.0133
PBM018															
PBM019	-0.0361	-0.0461	-0.0586	-0.0141	-0.0217	-0.0031	-0.0191	-0.0235	-0.0165	-0.0306	0.0180	-0.0048	0.0171	0.0084	-0.0011
PBM020	-0.0473	0.1364	0.0590	-0.0018	-0.0163	0.0508	-0.0520	-0.0767	0.0023	0.0050	0.0378	-0.0491	-0.0673	-0.0492	-0.0082
PBM021	-0.0694	0.1295	-0.0274	-0.0163	0.0599	0.0084	-0.0144	-0.0178	-0.0383	0.0178	0.0192	0.0050	0.0305	-0.0027	0.0104
PBM022	-0.0483	-0.0291	0.0100	-0.0074	0.0413	-0.0179	-0.0434	-0.0399	-0.0191	0.0054	0.0075	0.0368	0.0611	0.0220	0.0161
PBM023	-0.0917	0.0462	-0.0715	0.0685	0.0365	-0.0193	0.0043	-0.0348	0.0259	-0.0202	0.0115	-0.0093	0.0266	-0.0087	0.0198
PBM024	-0.0119	0.0819	0.0108	-0.0234	0.0042	-0.0118	0.0530	-0.0044	-0.0077	0.0068	-0.0146	0.0300	-0.0007	-0.0242	-0.0209
PBM025	-0.0627	0.0465	-0.0635	-0.0627	0.0035	-0.0183	0.0050	0.0728	-0.0025	0.0402	0.0237	-0.0125	0.0192	0.0268	-0.0110
PBM026	-0.1358	0.0091	0.0000	0.0431	0.0213	0.0089	-0.0190	0.0538	-0.0610	-0.1015	0.0113	0.0198	0.0223	-0.0215	0.0293
PBM027	-0.0684	0.0951	-0.1219	0.0780	0.0016	-0.0308	-0.0218	-0.0188	0.0086	0.0097	0.0189	-0.0042	0.0812	0.0170	-0.0084
PBM028															
PBM029	-0.0818	0.1134	-0.0241	0.0082	-0.0148	-0.0080	-0.0310	0.0195	0.0403	0.0443	0.0189	-0.0024	0.0027	0.0069	-0.0052
PBM030															
PBM031	-0.0338	-0.0707	0.0686	0.0293	0.0238	-0.0185	0.0158	-0.0249	-0.0099	0.0137	0.0269	0.0223	0.0091	-0.0104	-0.0064
PBM032															
PBM033	-0.0955	0.0395	0.1621	-0.0280	0.0159	0.0117	-0.0107	0.0340	-0.0077	0.0118	0.0193	-0.0204	-0.0107	0.0260	-0.0061
PBM034	-0.0104	0.0197	0.0574	-0.0419	0.0000	0.0011	0.0014	0.0299	0.0197	-0.0035	-0.0285	-0.0290	-0.0063	-0.0078	0.0204
PBM035	-0.0876	0.1064	-0.0115	0.0015	0.0237	0.0027	0.0054	0.0046	0.0361	0.0327	-0.0164	0.0142	-0.0085	-0.0082	-0.0108

Peripheral Retinal Profiles and Thickness in Anisomyopia

Enian Kallamata,[1] Nancy J. Coletta,[2] Gabriella M. Velonias,[1] Fuensanta A. Vera-Diaz[1]

[1]New England College of Optometry, Boston, MA, [2]MCPHS School of Optometry, Worcester, MA

New England College of Optometry

Poster 4364

Vera_DiazF@neco.edu

Background

In myopia, the globe expands in a prolate shape(1), causing stretching and subsequent thinning of the retina(2,3). Anisomyopia is the difference in the amount of myopia between the two eyes due to a difference in axial length(4).

There is limited data on the effects of anisomyopia on retinal thickness. Vincent et al (4) found that the more myopic eyes in anisometropia have thicker central foveas in Asian subjects. However there was no significant difference in Caucasian subjects. There is no available information on retinal thickness across the retina in anisomyopia.

Knowledge of the physical effects of anisomyopia will bring us one step closer to better understanding this condition.

Purpose

To evaluate retinal thickness variations across the central 56 degrees and compare between the two eyes of anisomyopes.

Hypothesis

Eyes with longer axial lengths will have a thinner retina at (1) the nasal foveal shoulder, (2) the temporal retina, and (3) nasal retina, and (4) will exhibit no difference in foveal pit thickness.

Methods

Subjects

- n=19 young adults (n=38 eyes) with anisomyopia (difference in SE of 1.00D or more); average SE difference: 1.79±1.01D.
- SE refractive error -0.13D to -11.38D, mean: -4.50±2.80D.
- AL 22.27 to 29.42 mm, mean: 25.17±1.64 mm.

Retinal Thickness

- OptoVUE OCT was used to measure retinal thickness across the central 56 degrees.
- Three OCT measurements: (1) fixating at a central target, (2) a target at +18deg, and (3) a target at -18deg eccentricity. Each 6-mm long B-scan provided 1020 samples of thickness.
- Using the full retinal thickness data, we analyzed the following dimensions:
  1. Foveal Pit thickness, defined as the thinnest point within the foveola (average 20 points).
  2. Nasal Foveal Shoulder thickness, defined as the thickest value nasal to the fovea (average of 20 points).
  3. Temporal Retina, defined as the slope and intercept of the area 10 to 28deg temporal to the fovea.
  4. Nasal Retina, defined as the average thickness of the nasal retina from 70 data points past the optic nerve head and up to 28deg eccentricity.

Axial Length

- Central and peripheral axial length measurements were taken using a LenStar LS900 (Haag Streit) on-axis, and at ± 30, 20, 16, 12, 8, and 4 degrees horizontally (average central AL difference: 0.68±0.41mm).

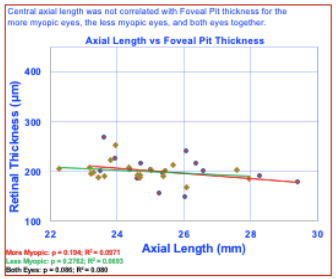
Statistics

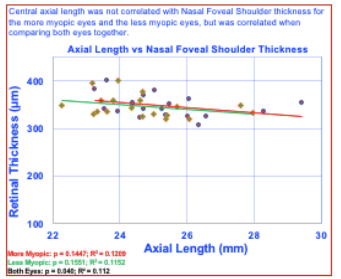
- Pearson Correlation statistical tests and two-sample t-tests were performed using Rstudio and SPSS.

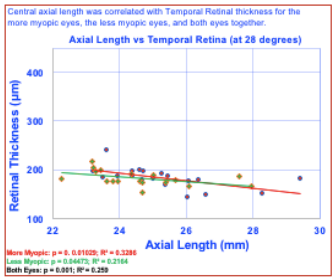
Discussion/Conclusions

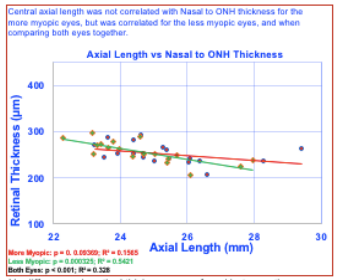
- Significant retinal thickness differences were found among individual eyes unlike the differences between the two eyes in anisomyopia.
- Retinal thickness differences between the more and less myopic eyes were found only in the area nasal to the ONH.
- Central retinal thickness does not appear to be affected by axial length.
- Further investigation of the physical effects of anisomyopia is essential to understanding its intricacies. Measuring subjects with a greater anisomyopic difference is the next step.

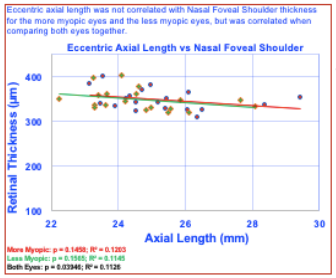
Results – Retinal Thickness











- No differences in retinal thickness were found between the more and less myopic eyes in anisomyopia (Foveal Pit: t=-0.02, p=0.98; Nasal Foveal Shoulder: t=0.06, p=0.95; Temporal Retina Thickness: t=0.08, p=0.94; or Nasal Retina thickness: t=-0.60, p=0.55).
- Comparing the difference between axial lengths and the thicknesses of the area nasal to the ONH of the more and less myopic eyes revealed a significant positive correlation (p=0.0364, R²=0.2328).

References

1. Shao SX. Regional Variation of Perifoveal Acuity, Retinal Thickness, and Retinal Contour in Myopia. Master's Thesis. 2013.
2. Chui TYP, Yap MKH, Chan HHL, Thibos LN. Retinal stretching limits peripheral visual acuity in myopia. Vision Res. 2005;45(5):593–605.
3. Coletta NJ, Watson T. Effect of myopia on visual acuity measured with laser interference fringes. Vision Res. 2000;46(5):636–51.
4. Vincent SJ, Collins MJ, Read SA, Carney LG. Retinal and choroidal thickness in myopic anisometropia. Invest Ophthalmol Vis Sci. 2013;54(4):2445–56.

Acknowledgements/Commercial Relationships

- American Academy of Optometry Research Career Development Award to Vera-Diaz.
- Enian Kallamata was supported by an NEI T35 EY007143 grant to the New England College of Optometry.
- None of the authors have commercial relationships.

8. Appendix 2

Peripheral retinal contours in emmetropia and myopia using biometric and optical quality parameters.

Gabriella M. Velonias,[1] Carles Otero,[2] Enian Kallamata,[1] Fuensanta A. Vera-Diaz[1]

[1]New England College of Optometry, Boston, MA [2]Anglia Ruskin University, Cambridge, UK

Poster 4836 - A0094

Vera_DiazF@neco.edu

Background

Knowledge of the peripheral retinal contour is important to understand refractive development and ultimately for the development of individualized myopia control methods.

The most commonly used method to compute retinal shape use peripheral eye length measurements. These give accurate results but oversimplified models, as they do not consider optical contributions, e.g., ocular indices or intraocular ray deviation[3,4].

While expensive and with limited resolution in the detection of retinal boundaries, MRI is the standard method to image retina shape and useful to validate alternative methods[3].

Peripheral refraction is also related to eye shape and has been suggested as a method to infer retinal contours[3].

None of these methods provide a comprehensive retinal contour model. Alternative methods that consider combining sensitive metrics of interaction between optics, refraction and biometric data are necessary.

Previous studies show less oblate and more prolate retinal shapes with increasing myopia, forming prolate ellipsoid surfaces that are greatest at the posterior pole[1,2]. Ocular surfaces, both the eye and retina, may be described by concoids with varying asphericity[1].

Purpose

To fit conical functions to biometric (axial length) and optical quality (monochromatic aberrations) data across the eye and analyze their correlations with myopia.

Hypotheses

- *We will find individual variability of retinal profiles and retinal image quality, with a refractive group effect.*
- *Significant effects of refractive error will be observed in the near peripheral retina, between 10-20 degrees eccentricity, where the human retina decoding system for blur appears to be.*

References

1. Verkicharla PK, Mathur A, Mallen EAH, Pope JM & Atchison DA. Eye shape and retinal shape, and their relation to peripheral refraction. Ophthalmic Physiol Opt. 2012;32:184-99.
2. Atchison DA, Pritchard N, Schmid KL, Scott DH, Jones CF, Pope JM. Shape of Retinal Surface in Emmetropia and Myopia. Invest Ophthalmol Vis Sci. 2005;46:2698-707
3. Verkicharla PK, Suheimat M, Pope JM, Segelstrband F, Mathur A, Schmid KL, et al. Validation of a partial coherence interferometry method for estimating retinal shape. Biomed Opt Express. 2015;6(9):3235.
4. Verkicharla PK, Suheimat M, Schmid KL & Atchison DA. Differences in retinal shape between East Asian and Caucasian eyes. Ophthalmic Physiol Opt 2017;37:275-83.
5. Chin MP, Chu PWK, Cheung AMY, Chan WHL. Human Electroretinal Responses to Grating Patterns and Defocus Changes by

Acknowledgements / Commercial Relationships

This research was supported by AAO-Career Development Award to Vera-Diaz. Gabriella Velonias was supported by NEI T35 program and additional funds provided by graduate studies program at New England College of Optometry. Commercial Relationships: No Commercial Relationships.

Methods

Subjects

- A group of young adults with healthy eyes, were divided in three refractive groups. Each group had no differences in BCVA or age.
  - * High Myopes, defined as SE between -5.00D and -12.00D: n=13, *mean central SE: -7.68±1.93D, central AL: 26.32±1.61mm*
  - * Low Myopes, defined as SE between -0.75D and -4.00D: n=24, *mean central SE: -2.45±1.02D, central AL: 24.17±0.75mm*
  - * Emmetropes, defined as SE between +0.75D and -0.50D: n=13, *mean central SE: -0.04±0.25 D, central AL: 23.45±0.60mm*

Biometry

- AL measurements (Lenstar LS900, Haag Streit) were taken across the central 60 degrees (at 13 eccentricities) of the transverse (axial) section.
- A conic function was used to fit retinal contours obtained from AL raw values, as described by Verkicharla et al, 2015 method[3]: $y=AL'_{p-r_{cv}}\sin\theta$ and $\Delta z=r_{cv}/(1-\cos\theta)+AL'_{p}\cos\theta-AL'_{a}$. The equation used:

$$y = C * \frac{(x)^2}{(1+\sqrt{1-(1+Q)*C^2*(x)^2})}$$

- Where y is surface sag co-ordinate, C is vertex curvature, Q is asphericity, x is co-ordinate along the X-axis.

Optical Quality

- Monochromatic aberrations (scanning peripheral aberrometer, VopticaSL) were obtained for every degree across 60 degrees of the transverse (axial) section while subjects looked at 4m.
- Optical quality was defined as the RMS (Root Mean Square) for each eye computed up to the 5th order for a 4mm pupil. RMS profiles were correlated with AL and also fitted using conic functions.
- A conic function was used to fit retinal contours obtained from aberrations raw values for parameters M, J0, J45, SA, RMSHoa, RMSall:

$$y = C * \frac{(x-x_0)^2}{(1+\sqrt{1-(1+Q)*C^2*(x-x_0)^2})} + y_0$$

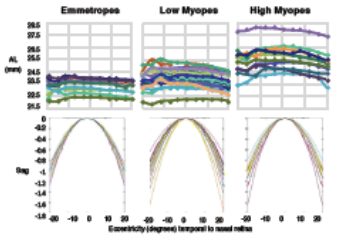
- Two-sample t-tests and regression analysis were applied to biometric

Conclusions

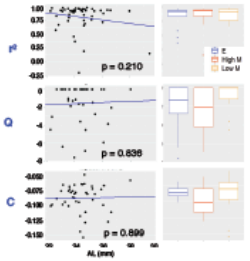
Both biometric and optical quality data across the retina may be accurately fitted to conic functions to evaluate retinal contours in emmetropia and myopia. Fitting conic functions to the RMS values across the retina simplifies the use of peripheral optical quality data and may be used in future studies as a peripheral optical quality metric.

Results

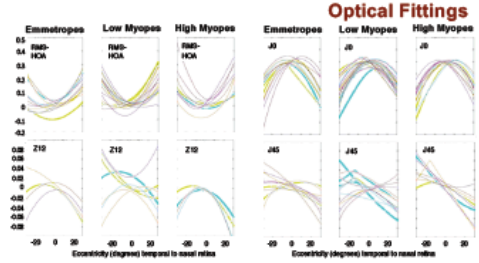
Biometric Data



- Accurate biometric fitting were achieved for the 41/50 subjects.
- Low Myopes significantly smaller Q than High Myopes (p = 0.049), indicating less prolate shape. No effect of refractive group in r^2 or C.
- No effect of AL in the goodness of fit (r^2), asphericity (Q) or curvature (C) of the retinal contour fittings using biometric parameters.

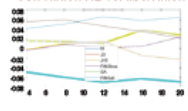


Optical Fittings

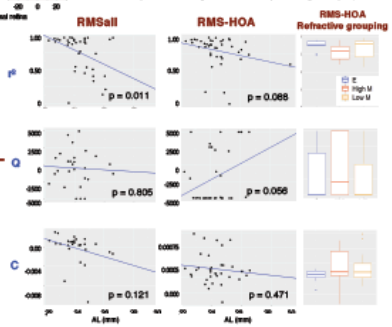


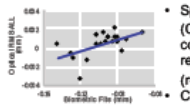
- Optical fittings for RMSall could be achieved for 27/50 and RMS-HOA for 36/50 subjects.
- With RMSall, goodness of fit (r^2) worsens with increased AL (p=0.01), with a high myopes having a higher r^2 (p=0.02) and greater curvature (C) (p=0.01) than emmetropes.
- There is a refractive error effect in the RMS-HOA fittings, with (r^2) worse for myopes (p=0.08) and more positive Q for high myopes (p=0.057).
- For asphericity (C), emmetropes have oblate and low myopes have hyperbolic shape, as seen in biometry data. High variability in high myopes.

Correlation AL vs. aberration



- RMSall and M best correlates with AL beyond 12deg eccentricity (r>0.6, p<0.05)
- J0 best correlates with AL within the central 8deg (r=0.56-0.60, p<0.05)





Correlation C optics vs. C biometry

- Spearman correlation of curvature (C) from biometric parameters compared to that of RMSALL revealed a positive relationship (r=0.441, p=0.018).
- Correlation of C from biometric parameters compared to that of RMSHOA revealed a small negative relationship (r=-0.311, p=0.05).

9. Literature Cited

1. Verkicharla PK, Suheimat M, Mallen EAH, Atchison DA. Influence of eye rotation on peripheral eye length measurement obtained with a partial coherence interferometry instrument. Ophthalmic Physiol Opt. 2014 Jan;34(1):82–8.
2. Hung GK, Mahadas K, Mohammad F. Eye growth and myopia development: Unifying theory and Matlab model. Comput Biol Med [Internet]. 2016;70:106–18.
3. Hashemi H, Fotouhi A, Yekta A, Pakzad R, Ostadimoghaddam H, Khabazkhoob M. Global and regional estimates of prevalence of refractive errors: Systematic review and meta-analysis. J Curr Ophthalmol [Internet]. 2018;30(1):3–22.
4. Saw SM, Gazzard G, Shin-Yen EC, Chua WH. Myopia and associated pathological complications. Vol. 25, Ophthalmic and Physiological Optics. 2005. p. 381–91.
5. Rose K. Quality of life in myopia. Br J Ophthalmol [Internet]. 2000;84(9):1031–4.
6. Fricke TR, Holden BA, Wilson DA, Schlenther G, Naidoo KS, Resnikoff S, et al. Global cost of correcting vision impairment from uncorrected refractive error. Bull World Health Organ. 2012;90(10):728–38.
7. Holden BA, Fricke TR, Wilson DA, Jong M, Naidoo KS, Sankaridurg P, et al. Global Prevalence of Myopia and High Myopia and Temporal Trends from 2000 through 2050. Ophthalmology [Internet]. 2016;123(5):1036–42.
8. Jaworski A, Gentle A, Zele AJ, Vingrys AJ, McBrien NA. Altered visual sensitivity in axial high myopia: A local postreceptoral phenomenon? Investig Ophthalmol Vis Sci. 2006;47(8):3695–702.
9. David T, Smye S, James T, Dabbs T. Time-dependent stress and displacement of the eye wall tissue of the human eye. Med Eng Phys [Internet]. 1997 Mar 1 [cited 2018 Apr

27];19(2):131–9.

10. David T, Smye S, Dabbs T, James T. A model for the fluid motion of vitreous humour of the human eye during saccadic movement. Phys Med Biol [Internet]. 1998 Jun [cited 2018 Apr 27];43(6):1385–99.
11. Hirata A, Negi A. Lacquer crack lesions in experimental chick myopia. Graefe's Arch Clin Exp Ophthalmol [Internet]. 1998 Jan 23 [cited 2018 Apr 27];236(2):138–45.
12. Williams K, Hammond C. High myopia and its risks. Community Eye Health. 2019;32(105):5–6.
13. Wallman J, Winawer J. Homeostasis of eye growth and the question of myopia. Neuron. 2004;43(4):447–68.
14. Raviola E, Wiesel TN. An Animal Model of Myopia. N Engl J Med [Internet]. 1985 Jun 20 [cited 2018 Apr 27];312(25):1609–15.
15. Smith EL 3rd, Hung LFLF. The role of optical defocus in regulating refractive development in infant monkeys. Vision Res. 1999 Apr;39(8):1415–35.
16. Wollensak G, Iomdina E. Long-term biomechanical properties of rabbit sclera after collagen crosslinking using riboflavin and ultraviolet A (UVA). Acta Ophthalmol. 2009;87(2):193–8.
17. Leotta AJ, Bowrey HE, Zeng G, Mcfadden SA. Temporal properties of the myopic response to defocus in the guinea pig. Ophthalmic Physiol Opt. 2013;33(3):227–44.
18. Tkatchenko T V., Shen Y, Braun RD, Bawa G, Kumar P, Avrutsky I, et al. Photopic visual input is necessary for emmetropization in mice. Exp Eye Res. 2013;115:87–95.
19. Zhu X, McBrien NA, Smith EL, Troilo D, Wallman J. Eyes in various species can shorten to compensate for myopic defocus. Investig Ophthalmol Vis Sci. 2013;54(4):2634–44.

20. Padmanabhan V, Shih J, Wildsoet CF. Constant light rearing disrupts compensation to imposed- but not induced-hyperopia and facilitates compensation to imposed myopia in chicks. Vision Res. 2007;47(14):1855–68.

21. Siegwart JT, Norton TT. Binocular lens treatment in tree shrews: Effect of age and comparison of plus lens wear with recovery from minus lens-induced myopia. Exp Eye Res [Internet]. 2010 Nov [cited 2018 Apr 27];91(5):660–9.

22. McBrien NA, Arumugam B, Metlapally S. The Effect of Daily Transient +4 D Positive Lens Wear on the Inhibition of Myopia in the Tree Shrew. Investig Opthalmology Vis Sci [Internet]. 2012 Mar 21 [cited 2018 Apr 27];53(3):1593.

23. Jaeken B, Artal P. Optical quality of emmetropic and myopic eyes in the periphery measured with high-angular resolution. Investig Ophthalmol Vis Sci. 2012;53(7):3405–13.

24. Rosenblum WM, Christensen JL. III Objective and Subjective Spherical Aberration Measurements of the Human Eye. Prog Opt [Internet]. 1976 Jan 1 [cited 2018 Apr 27];13:69–91.

25. Howland HC, Howland B. A subjective method for the measurement of monochromatic aberrations of the eye. J Opt Soc Am. 1977;67(11):1508–18.

26. Walsh G, Charman WN, Howland HC. Objective technique for the determination of monochromatic aberrations of the human eye. J Opt Soc Am A [Internet]. 1984;1(9):987. Available from: http://josaa.osa.org/abstract.cfm?URI=josaa-1-9-987

27. Campbell MCW, Harrison EM, Simonet P. Psychophysical measurement of the blur on the retina due to optical aberrations of the eye. Vision Res [Internet]. 1990 Jan 1 [cited 2018 Apr 27];30(11):1587–602.

28. Porter J, Guirao A, Cox IG, Williams DR. Monochromatic aberrations of the human eye in a large population. J Opt Soc Am A [Internet]. 2001;18(8):1793.

29. Thibos LN, Bradley A, Liu T, López-Gil N. Spherical aberration and the sign of defocus. Optom Vis Sci. 2013;90(11):1284–91.

30. Kruger, P., & Pola, J. (1986). Stimuli for accommodation: blur, chromatic aberration and size. Vision Research, 26(6): 957-971.

31. Fisher, S.K., & Ciuffreda, K.J. (1988). Accommodation and apparent distance. Perception, 17(5): 609-621.

32. Mather, G., & Smith, D. R. (2002). Blur discrimination and its relation to blur-mediated depth perception. Perception, 31(10), 1211–1219.

33. Maiello, G., Chessa, M., Solari, F., & Bex, P.J. (2014). Simulated disparity and peripheral blur interact during binocular fusion. Journal of Vision, 14(8): 13, 1-14.

34. Liang JZ, Williams DR. Aberrations and retinal image quality of the normal human eye. J Opt Soc Am a-Optics Image Sci Vis. 1997;14(11):2873–83.

35. de Gracia P, Dorronsoro C, Gambra E, Marin G, Hernández M, Marcos S. Vision Res. Combining coma with astigmatism can improve retinal image over astigmatism alone. 2010 Sep 15;50(19):2008-14.

36. Vera-Diaz FA, Otero C, Bex PJ. Effect of monochromatic aberrations on suprathreshold and threshold discrimination tasks. Investigative Ophthalmology and Visual Science 2018;58: ARVO E-Abstract A0315.

37. Smith EL, Ramamirtham R, Qiao-Grider Y, Hung LF, Huang J, Kee CS, et al. Effects of foveal ablation on emmetropization and form-deprivation myopia. Investig Ophthalmol Vis Sci. 2007;48(9):3914–22.

38. Huang J, Hung LF, Smith EL. Effects of foveal ablation on the pattern of peripheral refractive errors in normal and form-deprived infant rhesus monkeys (Macaca mulatta). Investig Ophthalmol Vis Sci. 2011;52(9):6428–34.

39. Smith EL 3rd, Hung L-F, Huang J, Arumugam B. Effects of local myopic defocus on refractive development in monkeys. Optom Vis Sci. 2013;90(11):1176–86.

40. Rempt F, Hoogerheide J, Hoogenboom WPH. Peripheral Retinoscopy and the Skiagram. Ophthalmologica [Internet]. 1971 [cited 2018 Apr 27];162(1):1–10.

41. Hoogerheide J, Rempt F, Hoogenboom WPH. Acquired Myopia in Young Pilots. Ophthalmologica [Internet]. 1971 [cited 2018 Apr 27];163(4):209–15.

42. Nathan, J., Kiely, P., Gillard Crewther, S., & Crewther, D. (1985). Disease-associated visual image degradation and spherical refractive errors in children. American Journal of Optometry & Physiological Optics, 62(10): 680-688.

43. Knight-Nanan, D., & O'Keefe, M. (1996). Refractive outcome in eyes with retinopathy of prematurity treated with cryotherapy or diode laser: 3 year follow up. British Journal of Ophthalmology. 80, 998-1001.

44. Atchison DA, Li SM, Li H, Li SY, Liu LR, Kang MT, et al. Relative peripheral hyperopia does not predict development and progression of myopia in children. Investig Ophthalmol Vis Sci. 2015;56(10):6162–70.

45. Rosén R, Lundström L, Unsbo P, Atchison DA. Have we misinterpreted the study of Hoogerheide et al. (1971)? Optom Vis Sci. 2012;89(8):1235–7.

46. Lee T-T, Cho P. Relative peripheral refraction in children: twelve-month changes in eyes with different ametropias. Ophthalmic Physiol Opt [Internet]. 2013 May [cited 2018 Apr 27];33(3):283–93.

47. Sng CCA, Lin XY, Gazzard G, Chang B, Dirani M, Lim L, et al. Change in peripheral refraction over time in Singapore Chinese children. Investig Ophthalmol Vis Sci. 2011;52(11):7880–7.

48. Smith EL, Hung LF. The role of optical defocus in regulating refractive development in infant monkeys. Vision Res. 1999;39(8):1415–35.

49. Wallman J, Gottlieb MD, Rajaram V, Fugate-Wentzek LA. Local retinal regions control local eye growth and myopia. Science [Internet]. 1987 Jul 3 [cited 2017 May 31];237(4810):73–7.

50. Atchison DA, Pritchard N, Schmid KL. Peripheral refraction along the horizontal and vertical visual fields in myopia. Vision Res. 2006;46(8–9):1450–8.

51. Chin MP, Chu PHW, Cheong AMY, Chan HHL. Human electroretinal responses to grating patterns and defocus changes by global flash multifocal electroretinogram. PLoS One [Internet]. 2015;10(4):1–21.

53. Flitcroft DI. The complex interactions of retinal, optical and environmental factors in myopia aetiology. Prog Retin Eye Res. 2012;31(6):622–60.

55. Aigbe S, Panorgias T, Jeong E, Otero Molins C, Bex PJ, Vera-Diaz FA . Cross-Retinal ERG Responses to Simulated Optical Blur in Myopia. Investigative Ophthalmology and Visual Science. 2019 ;59:ARVO E-Abstract A0085.

56. Lundström L, Mira-Agudelo A, Artal P, Lundstrom L, Mira-Agudelo A, Artal P. Peripheral optical errors and their change with accommodation differ between emmetropic and myopic eyes. J Vis. 2009;9(6):17.1-11.

57. Mathur A, Atchison D a, Charman WN. Effect of accommodation on peripheral ocular aberrations. J Vis [Internet]. 2009;9(2009):1–11.

58. Hartwig A, Charman WN, Radhakrishnan H. Accommodative response to peripheral stimuli in myopes and emmetropes. Ophthalmic Physiol Opt. 2011;31(1):91–9.

59. Kerber KL, Thorn F, Bex PJ V-DF. Peripheral contrast sensitivity and attention in myopia. Vis Res 2016 Aug;12549-54.

60. Atchison DA, Jones CE, Schmid KL, Pritchard N, Pope JM, Strugnell WE, et al. Eye Shape in Emmetropia and Myopia. 2004;3380–6.

61. Nagra M, Gilmartin B, Thai NJ LN. Determination of retinal surface area. J Anat 2017 Sep;231(3)319-324.

62. Vera-Diaz FA. The Importance of Measuring Axial Length. Review of Myopia Management.

63. Gwiazda J, Deng L, Norton T, Manny R, the COMET group. Seasonal progression in the Correction of Myopia Evaluation Trial (COMET) cohort. Invest Ophthalmol Vis Sci. 2014; 55(2):752-8.

64. Vohra SB, Good PA. Altered globe dimensions of axial myopia as risk factors for penetrating ocular injury during peribulbar anaesthesia. Br J Anaesth [Internet]. 2000;85(2):242–5.

65. Deller, J., O'Connor, A., & Sorsby, A. (1947). X-Ray Measurement of the Diameters of the Living Eye. Proceedings of the Royal Society of London. Series B, Biological Sciences, 134(877), 456-467.

66. Zhou X-D, Wang F-R, Zhou S-Z, Shi J-S. A computed tomographic study of the relation between ocular axial biometry and refraction. In: Tokoro T, ed. Myopia Updates: Proceedings of the 6th International Conference of Myopia. New York: Springer; 1998; 112-11.

67. Atchison DA, Pritchard N, Schmid KL, Scott DH, Jones CE, Pope JM. Shape of the Retinal Surface in Emmetropia and Myopia. 2005;2698–707.

68. Clark CA, Elsner AE KB. Eye shape using partial coherence interferometry, autorefraction, and SD-OCT. Optom Vis Sci 2015 Jan;92(1)115-22.

69. Fedtke C, Ehrmann K, Holden BA. A review of peripheral refraction techniques. Optom Vis Sci 2009;86:429Y46.

70. Verkicharla PK, Mathur A, Mallen EAH, Pope JM, Atchison DA. Eye shape and retinal shape , and their relation to peripheral refraction. 2012;32:184–99.

71. Verkicharla PK, Mallen E a H, Atchison D a. Repeatability and Comparison of Peripheral Eye Lengths With Two Instruments. Optom Vis Sci. 2013;90(3):215–22.

72. Atchison DA, Pritchard N, White SD, Griffiths AM. Influence of age on peripheral refraction. 2005;45:715–20.

73. Atchison DA, Charman WN. Can Partial Coherence Interferometry be Used to Determine Retinal Shape? Optom Vis Sci [Internet]. 2011 May [cited 2018 Apr 27];88(5):E601–7.

74. Verkicharla PK, Suheimat M, Pope JM, Sepehrband F, Mathur A, Schmid KL, et al. Validation of a partial coherence interferometry method for estimating retinal shape. Biomed Opt Express [Internet]. 2015;6(9):3235.

75. Backhouse S, Fox S, Ibrahim B & Phillips JR. Peripheral refraction in myopia corrected with spectacles versus contact lenses. Ophthalmic Physiol Opt 2012, 32, 294–303.

76. Logan NS, Gilmartin B, Wildsoet CF, Dunne MCM. Posterior retinal contour in adult human anisomyopia. Investig Ophthalmol Vis Sci. 2004;45(7):2152–62.

77. Schmid G S. Association between Retinal Steepness and Central Myopic Shift in Children. Optom Vis Sci June 2011 - Vol 88 - Issue 6 - p 684-690.

79. Ehsaei A, Chisholm CM, Pacey IE, Mallen EA. Off-axis partial coherence interferometry in myopes and emmetropes. Ophthalmic Physiol Opt. 2013;33(1):26–34.

80. Verkicharla PK, Suheimat M, Pope JM, Sepehrband F, Mathur A, Schmid KL, et al. Validation of a partial coherence interferometry method for estimating retinal shape. Biomed Opt Express. 2015;6(9):3235.

81. Verkicharla PK, Suheimat M, Schmid KL, Atchison DA. Differences in retinal shape between East Asian and Caucasian eyes. 2017;37:275–83.

82. Verkicharla PK, Suheimat M, Schmid KL, Atchison DA. Differences in retinal shape between East Asian and Caucasian eyes. Ophthalmic Physiol Opt [Internet]. 2017;37(3):275–83.

83. Mutti DO, Sholtz RI, Friedman NE, Zadnik K. Peripheral Refraction and Ocular Shape in Children. 2000;41(5):1022–30.

84. Mutti DO, Sinnott LT, Reuter KS, Walker MK, Berntsen DA, Jones-Jordan LA, et al. Peripheral refraction and eye lengths in myopic children in the bifocal lenses in nearsighted kids (BLINK) study. Transl Vis Sci Technol. 2019;8(2).

85. Faria-Ribeiro M, Queirós A, Lopes-Ferreira D, Jorge J G-MJ. Peripheral refraction and retinal contour in stable and progressive myopia. Optom Vis Sci 2013 Jan;90(1)9-15.

87. Cruickshank FE, Logan NS. Optical 'dampening' of the refractive error to axial length ratio: implications for outcome measures in myopia control studies. Ophthalmic Physiol Opt. 2018;38(3):290–7.

88. Smith EL 3rd, Hung LFLF. The role of optical defocus in regulating refractive development in infant monkeys. Vision Res. 1999;39(8):1415-1435.

89. Flitcroft DI. Emmetropisation and the aetiology of refractive errors. Eye [Internet].

2014;28(2):169–79.

90. Philip K, Sankaridurg P, Holden B, Ho A, Mitchell P. Influence of higher order aberrations and retinal image quality in myopisation of emmetropic eyes. Vision Res [Internet]. 2014;105:233–43.

91. Vincent SJ, Read SA. Clinical and Experimental. Higher order aberrations , refractive error development and myopia control : a review. 2020;(January):68–85.

92. Tian Y, Tarrant J, Wildsoet CF. Optical and biometric characteristics of anisomyopia in human adults. Ophthalmic Physiol Opt. 2011;31(5):540–9.

93. Julie-Anne Little, Sara J. McCullough, Karen M. M. Breslin, Kathryn J. Saunders; Higher Order Ocular Aberrations and Their Relation to Refractive Error and Ocular Biometry in Children. Invest. Ophthalmol. Vis. Sci. 2014;55(8):4791-4800.

94. Marcos, S. (2002). The sources of optical aberrations in myopic eyes. Fort Lauderdale, IOVS: ARVO.

96. Mathur, A., Atchison, D. A., & Charman, W. N. (2009). Myopia and peripheral ocular aberrations. Journal of Vision, 9(10):15, 1–12.

97. Kirwan, C., O'Keefe, M., & Soeldner, H. (2006). Higher-order aberrations in children. American Journal of Ophthalmology, 141(1), 67–70.

98. Radhakrishnan, H., Pardhan, S., Calver, R. I., & O'Leary, D. J. (2004). Effect of positive and negative defocus on contrast sensitivity in myopes and non-myopes. Vision Research, 44(16), 1869–1878.

99. Cheng X, Bradley A, Hong X, Thibos LN. Relationship between refractive error and monochromatic aberrations of the eye. Optom Vis Sci. 2003 Jan; 80(1):43-9.

100. Atchison DA, Schmid KL, Pritchard N. Neural and optical limits to visual performance in

myopia. Vision Res. 2006;46(21):3707–22.

101. Zhang N, Yang XB, Zhang WQ, Liu LQ, Dong GJ, Chen TW, et al. Relationship between higher-order aberrations and myopia progression in schoolchildren: A retrospective study. Int J Ophthalmol. 2013;6(3):295–9.

102. Lau JK, Vincent SJ, Collins MJ, Cheung SW, Cho P. Ocular higher-order aberrations and axial eye growth in young Hong Kong children. Sci Rep [Internet]. 2018;8(1):2–11.

103. Thibos LN, Bradley A, L??pez-Gil N. Modelling the impact of spherical aberration on accommodation. Ophthalmic Physiol Opt. 2013;33(4):482–96.

104. Shih YF, Lin LL, Peng Y, Ko LS. Clinical observations on occlusion myopia. Taiwan Yi Xue Hui Za Zhi 1989;88:164Y8.

105. Rabin J, Van Sluyters RC, Malach R. Emmetropization: a vision- dependent phenomenon. Invest Ophthalmol Vis Sci 1981;20:561Y4.

106. Atchison, D. A. (2006b). Higher order aberrations across the horizontal visual field. Journal of Biomedical Optics, 11, 034026.

107. Atchison D a, Scott DH. Monochromatic aberrations of human eyes in the horizontal visual field. J Opt Soc Am A Opt Image Sci Vis. 2002;19(11):2180–4.

108. Navarro, R. Moreno, E. Dorronsoro, C. (1998). Monochromatic aberrations and point-spread functions of the human eye across the visual field. Journal of the Optical Society of America A, Optics, Image Science, and Vision, 15, 2522–2529.

109. Mathur, A., Atchison, D. A., & Scott, D. H. (2008). Ocular aberrations in the peripheral visual field. Optics Letters, 33, 863–865.

110. Atchison, D. A. (2006a). Errata: Higher order aberrations across the horizontal visual field. Journal of Biomedical Optics, 11, 059801.

111. Bart Jaeken, Sandra Mirabet, José María Marín, Pablo Artal; Comparison of the Optical Image Quality in the Periphery of Phakic and Pseudophakic Eyes. Invest. Ophthalmol. Vis. Sci. 2013;54(5):3594-3599.

112. Iskander DR. Computational aspects of the visual Strehl ratio. Optom Vis Sci. 2006;83(1):57–9.

113. J. z; Wavefront Aberrations Measurement Incorporating the Stiles-Crawford Effect . Invest. Ophthalmol. Vis. Sci. 2003;44(13):2572.

115. Analysis A, Manual U. User Manual User Manual. 2012;(1):1–148.

116. Jaeken B, Lundström L, Artal P. Fast scanning peripheral wave-front sensor for the human eye.

117. Bart Jaeken PAS. Instrument for rapid measurement of the optical properties of the eye in the entire field of vision. 2011.

118. Lan W, Lin Z, Yang Z, Artal P. Two-dimensional Peripheral Refraction and Retinal Image Quality in Emmetropic Children. Sci Rep. 2019;9(1):1–9.

119. Tabernero, J. & Schaeffel, F. More Irregular Eye Shape in Low Myopia Than in Emmetropia. Invest. Ophthalmol. Vis. Sci. 50, 4516–4522 (2009).

120. Osuagwu UL, Suheimat M, Atchison DA. Peripheral aberrations in adult hyperopes, emmetropes and myopes. Ophthalmic Physiol Opt. 2017;37(2):151–9.

121. Mathur A, Atchison DA, Tabernero J, Article O. Effect of Age on Components of Peripheral Ocular Aberrations. Optom Vis Sci [Internet]. 2012;89(7):E967-76.

122. Llorente L, Barbero S, Cano D, Dorronsoro C, Marcos S. Myopic versus hyperopic eyes: Axial length, corneal shape and optical aberrations. J Vis. 2004;4(4):288–98.

123. Otero C, Kallamata E, Velonias G, Tabernero J, Vera-Diaz FA. Retinal contour and

peripheral optical quality interactions in isomyopia and anisomyopia. Investigative Ophthalmology and Visual Science 2018;58: ARVO E-Abstract 4937.

124. Roy A, Kar M, Mandal D, Ray RS, Kar C. Variation of Axial Ocular Dimensions with Age, Sex, Height, BMID, and Their Relation to Refractive Status. J Clin Diagn Res. 2015;9(1): AC01-AC4